



1 Constraints on Hadean zircon protoliths from oxygen 2 isotopes, Ti-thermometry, and rare earth elements

3 **Dustin Trail**

4 *Department of Geological Sciences and Center for Astrobiology, University of Colorado, Boulder, Colorado 80309-0399,*
5 *USA*

6 *Now at Department of Earth and Environmental Sciences, Rensselaer Polytechnic Institute, Troy, New York 12180,*
7 *USA (traild@rpi.edu)*

8 **Stephen J. Mojzsis**

9 *Department of Geological Sciences and Center for Astrobiology, University of Colorado, Boulder, Colorado 80309-0399,*
10 *USA*

11 **T. Mark Harrison**

12 *Research School of Earth Sciences, Australian National University, Canberra, ACT 0200, Australia*

14 *Department of Earth and Space Sciences and Institute of Geophysics and Planetary Physics, University of California,*
15 *Los Angeles, California 90095, USA*

16 **Axel K. Schmitt**

17 *Department of Earth and Space Sciences and Institute of Geophysics and Planetary Physics, University of California,*
18 *Los Angeles, California 90095, USA*

19 **E. Bruce Watson**

20 *Department of Earth and Environmental Sciences, Rensselaer Polytechnic Institute, Troy, New York 12180, USA*

21 **Edward D. Young**

22 *Department of Earth and Space Sciences and Institute of Geophysics and Planetary Physics, University of California,*
23 *Los Angeles, California 90095, USA*

24 [1] We report zircon oxygen isotope ratios and reconnaissance Ti-in-zircon concentrations, guided by
25 cathodoluminescence image studies, for detrital zircons up to 4.34 Ga from the Narryer Gneiss Complex of
26 Western Australia. Zircon oxygen isotope results bolster the view that some Hadean (>3.85 Ga) zircon
27 source melts were enriched in heavy oxygen, a sensitive proxy for melt contamination by sediments altered
28 in liquid water. Zircon crystallization temperatures calculated from Ti concentration in pre-3.8 Ga zircons
29 yield values around 680°C in all cases except for one lower value in a 4.0 Ga grain. Elevated zircon $\delta^{18}\text{O}$
30 values reported here and elsewhere, combined with low minimum-melt crystallization temperatures, and
31 analysis of zircon/melt partitioning of rare earth elements (REEs) provide mutually consistent lines of
32 evidence that the Hadean Earth supported an evolved rock cycle which included formation of granitic
33 water-saturated melts, extensive continental crust, hydrosphere-lithosphere interactions, and sediment
34 recycling within the first 150 million years of planet formation.

35 **Components:** 14,639 words, 6 figures, 3 tables.

36 **Keywords:** Hadean; crust; ion microprobe; oxygen; zircon thermometry; rare earth elements.

37 **Index Terms:** 1009 Geochemistry: Geochemical modeling (3610, 8410); 1020 Geochemistry: Composition of the
 38 continental crust; 1065 Geochemistry: Major and trace element geochemistry; 1041 Geochemistry: Stable isotope
 39 geochemistry (0454, 4870); 1042 Geochemistry: Mineral and crystal chemistry (3620).

40 **Received** 17 August 2006; **Revised** 16 February 2007; **Accepted** 15 March 2007; **Published** XX Month 2007.

41 Trail, D., S. J. Mojzsis, T. M. Harrison, A. K. Schmitt, E. B. Watson, and E. D. Young (2007), Constraints on Hadean zircon
 42 protoliths from oxygen isotopes, Ti-thermometry, and rare earth elements, *Geochem. Geophys. Geosyst.*, 8, XXXXXX,
 43 doi:10.1029/2006GC001449.

45 1. Introduction

46 [2] In the apparent absence of a continuous Hadean
 47 (pre-3.85 Ga [Bleeker, 2004]) geologic record on
 48 Earth, information bearing on the formation and
 49 evolution of the earliest crust has traditionally
 50 relied on geodynamical model studies [Reymer
 51 and Schubert, 1985], and broad comparisons with
 52 lunar data [Tera et al., 1974]. Additional inferences
 53 have been made from pervasively altered [Moorbath
 54 et al., 1997; Sano et al., 1999] circa 4.0 Ga granitoid-
 55 gneiss terranes [Bowring and Williams, 1999;
 56 Izuka et al., 2006] and geochemical analyses of
 57 pre-4.0 Ga detrital zircons from Western Australia
 58 [e.g., Maas et al., 1992; Mojzsis et al., 2001;
 59 Watson and Harrison, 2005]. Abundant occurren-
 60 ces of detrital Hadean zircons that comprise up to
 61 several percent of the total zircon population in
 62 some quartzitic metasediments have been docu-
 63 mented from the Mount Narryer (MN) [Froude et
 64 al., 1983] and Jack Hills (JH) [Compston and
 65 Pidgeon, 1986] localities of the Narryer Gneiss
 66 Complex (NGC), at the northwestern edge of the
 67 Yilgarn Craton in Western Australia [e.g., Pidgeon
 68 and Wilde, 1998]. The Hadean zircons provide an
 69 excellent resource to explore the earliest Earth since
 70 zircon is refractory and resistant to chemical alter-
 71 ation and physical breakdown during weathering.
 72 Non-metamict crystals can serve as robust reposi-
 73 tories of Pb* [Cherniak and Watson, 2000], oxygen
 74 isotopes [Valley, 2003], Hf isotopes [Cherniak et
 75 al., 1997] and radiogenic Xe [Turner et al., 2004]
 76 (compare to Nd isotopes [Caro et al., 2006]) even
 77 in crystals that predate the start of the known
 78 terrestrial rock record [e.g., Harrison et al., 2005a].

79 [3] If zircon retains primary oxygen isotopes from
 80 the time of crystallization, such values can be used
 81 to place broad constraints on Hadean zircon mag-
 82 matic sources [e.g., Mojzsis et al., 2001; Cavosie et

al., 2005]. This is because empirically-derived 83
 zircon/melt oxygen isotopic fractionation factors 84
 [Valley et al., 2003] can constrain bulk protolith 85
 magma sources and magmatic evolution [Taylor, 86
 1968; Taylor and Sheppard, 1986]. Zircon oxygen 87
 isotope compositions occupy a large range of 88
 $^{18}\text{O}/^{16}\text{O}$ ratios [Valley et al., 2005]. It is generally 89
 accepted that deviation of crustal zircon from man- 90
 tle $\delta^{18}\text{O}_{\text{VSMOW}}$ values ($+5.3 \pm 0.3\%$ [Valley, 2003]) 91
 indicates its source melts were in chemical com- 92
 munication with a reservoir enriched (or depleted) 93
 in ^{18}O , and the only natural system that can impart 94
 such signatures is liquid water interacting with crust 95
 at or near Earth's surface. As reviewed by Valley et 96
 al. [2005], magmatic zircon $\delta^{18}\text{O}$ values derived 97
 from remelted hydrothermally altered rhyolites 98
 from Yellowstone are as low as -0.4% , and meas- 99
 urements as high as $+13.5\%$ have been reported 100
 from a quartz monzonite from the Frontenac Arch 101
 Crow Lake Pluton in Ontario. Non-magmatic $\delta^{18}\text{O}$ 102
 zircon values as low as -11% are documented for 103
 hydrothermally altered rocks from the Dabie-Sulu 104
 orogen in China that later underwent ultra-high- 105
 pressure metamorphism [Zheng et al., 2003]. Oxy- 106
 gen isotope values up to $+15\%$ for circa 3650 Ma 107
 metamorphic zircons in granulite facies supracrus- 108
 tal enclaves (quartz-garnet biotite schists) from the 109
 Færinghavn terrane of southern West Greenland 110
 [Cates and Mojzsis, 2006], and from a discordant 111
 overgrowth of a Hadean Jack Hills zircon [Mojzsis 112
 et al., 2001] have also been reported. 113

114 [4] Oxygen-18 enrichments relative to mantle val- 114
 ues measured for core regions in pre-3.8 Ga zircons 115
 have been interpreted by a number of workers to 116
 indicate an evolved rock cycle and derivation from 117
 "S-type" granitoid melts in the Hadean [Mojzsis et 118
 al., 2001; Peck et al., 2001; Valley et al., 2002; 119
 Cavosie et al., 2005]. However, alternative views 120
 have been proposed that provide different explan- 121

122 ations for the Hadean zircon data. For example,
 123 oxygen isotope analyses of eight pre-4.2 Ga
 124 zircons by *Nemchin et al.* [2006a] yielded values
 125 broadly within the terrestrial mantle field and led
 126 them to conclude that there was insufficient evi-
 127 dence for a “cool early Earth” between ~ 4.4 –
 128 4.0 Ga as advocated by *Valley et al.* [2002].
 129 Instead, *Nemchin et al.* [2006a] drew generic
 130 parallels with their Jack Hills zircon analyses and
 131 results from a separate study of lunar zircons
 132 [*Nemchin et al.*, 2006b] to presume that oxygen
 133 isotopes in zircons provide no unique evidence for
 134 crust-hydrosphere interactions prior to ~ 4.0 Ga.

135 [5] Titanium concentration in zircon ($[\text{Ti}]_{\text{zircon}}$) is a
 136 geochemical tracer with potential to constrain
 137 zircon crystallization temperature. Recent $[\text{Ti}]_{\text{zircon}}$
 138 results for 4.35–4.0 Ga Jack Hills zircons indicate
 139 formation temperatures that cluster around 680°C
 140 [*Watson and Harrison*, 2005, 2006]. The $[\text{Ti}]_{\text{zircon}}$
 141 thermometer presupposes coexistence of rutile
 142 (essentially pure TiO_2) with zircon at crystalliza-
 143 tion. On the basis of measured $[\text{Ti}]_{\text{zircon}}$, an equi-
 144 librium constant can be calculated from the activity
 145 of TiO_2 in zircon by assuming an activity of rutile
 146 equal to ~ 1 [*Watson and Harrison*, 2005]. The
 147 $[\text{Ti}]_{\text{zircon}}$ thermometer has been calibrated experi-
 148 mentally for high (1025 – 1450°C) temperatures,
 149 and natural zircons have been used for crystalliza-
 150 tion temperatures of $\sim 580^\circ\text{C}$ – 1170°C [*Watson et al.*,
 151 2006]. The retention of tetravalent Ti in zircon is
 152 aided by the fact that it substitutes without charge
 153 compensation most favorably into the Si^{4+} site
 154 [*Harrison et al.*, 2005b; *Ferry and Watson*, 2007].

155 [6] *Maas et al.* [1992] reported rare earth element
 156 (REE) patterns in individual JH and MN zircons
 157 which show that some grains are markedly enriched
 158 in LREE contents and are similar to zircons from
 159 Phanerozoic diorites and granites. Follow-up studies
 160 presented $\delta^{18}\text{O}$ data in concert with REE data,
 161 showing high $\delta^{18}\text{O}$ values as well as enriched
 162 LREEs, which substantiate earlier conclusions that
 163 the chemistry of JH grains are consistent with zircons
 164 derived from granitoid-type source rocks [*Peck et al.*,
 165 2001; cf. *Coogan and Hinton*, 2006]. In another
 166 study, trace element patterns and U concentrations
 167 of detrital zircons from Mount Narryer were used to
 168 argue that these particular grains were derived from
 169 evolved granitic rocks [*Crowley et al.*, 2005].

170 [7] Geochemical tracers in zircon such as oxygen
 171 isotope ratios, Ti thermometry, and analysis of
 172 zircon/melt partitioning of REEs can be used to
 173 constrain zircon paragenesis in the absence of their
 174 parent rocks. For example, were Hadean zircon

protoliths dominantly of low temperature granite- 175
 type or instead the product of relatively high- 176
 temperature mafic/ultramafic melts? Here, we 177
 present new oxygen isotope data for 89 pre-3.8 Ga 178
 grains previously characterized by U-Pb ion micro- 179
 probe geochronology [*Harrison et al.*, 2005a]. In 180
 addition, multiple $\text{Ti}_{\text{zircon}}$ measurements were made 181
 for a subset ($n = 13$) of the pre-3.8 Ga grains. Our 182
 new Ti concentrations for zircons correspond to 183
 temperatures around 680°C , consistent with granite 184
 formation under conditions akin to wet minimum- 185
 melts [*Watson and Harrison*, 2005]. Moreover, our 186
 REE modeling demonstrates that Hadean zircons 187
 are dominantly of felsic magmatic provenance. 188
 These observations complement recent Hf isotope 189
 data from individual Hadean zircons that appear to 190
 be consistent with the establishment of significant 191
 continental crust and active plate boundary process- 192
 es within the first 150 million years of Earth 193
 formation [*Harrison et al.*, 2005a, 2006]. 194

2. Samples and Methods 195

[8] Collection localities and preparation techniques 196
 for samples JH992, ANU, JH0101 (Jack Hills), and 197
 MN0102 (Mount Narryer) are discussed in detail 198
 elsewhere (D. Trail et al., Post-crystallization events 199
 documented in Hadean zircons, submitted to 200
Geochimica Cosmochimica Acta, 2006; hereinafter 201
 referred to as Trail et al., submitted manuscript, 202
 2006). Briefly, JH992 [*Mojzsis et al.*, 2001] and 203
 ANU [*Harrison et al.*, 2005a] samples were col- 204
 lected from the original locality ($\text{S}26^\circ 10.09'$, $\text{E}116^\circ$ 205
 $59.39'$) where pre-4.0 Ga Jack Hills zircons were 206
 first discovered [*Compston and Pidgeon*, 1986]. 207
 Additionally, a new sample was included from a 208
 separate rock outcrop (JH0101) ~ 250 m west along 209
 strike from the JH992 locality, which preserved 210
 stream bedform and scour features with bands rich 211
 in heavy minerals. Mount Narryer sample MN0102 212
 ($\text{S}26^\circ 30.90'$, $\text{E}116^\circ 22.80'$) was a ~ 3 kg specimen 213
 that contained cm-scale clasts of banded iron-formation 214
 (BIF) visible in hand sample. Zircons were 215
 concentrated using standard heavy liquid techni- 216
 ques. Sieved samples were first treated with hand 217
 magnet and isodynamic Frantz magnetic separator 218
 (~ 1.5 A) to remove magnetic fractions prior to 219
 heavy liquid separations. After cleaning in acetone 220
 and deionized water ($\text{DI H}_2\text{O}$), zircons picked from 221
 the heavy mineral separates were mounted on 222
 double-sided adhesive tape and cast in 2.5 cm 223
 epoxy discs. Grain cross sections of individual 224
 zircons exposed during polishing were brought to 225
 optical finish using $0.05 \mu\text{m}$ alumina paste. 226

2.1. Zircon Oxygen Isotope Determination by Ion Microprobe Multicollection

[9] All high spatial resolution $\delta^{18}\text{O}$ zircon determinations were made using the UCLA CAMECA ims 1270 high-resolution ion microprobe in Faraday multicollection mode [e.g., *Mojzsis et al.*, 2001; *Booth et al.*, 2005] with regular monitoring of background count rates on the detectors. In all analyses a liquid nitrogen cold finger was used to remove trace condensable gases from the sample chamber. A ~ 5 nA Cs^+ beam was focused to a ~ 20 μm spot and 10 keV secondary ions were admitted to the mass spectrometer after passing through a 30 eV energy slit. Mass spectrometer entrance and exit slits were tuned to a mass resolving power of ~ 2400 to resolve hydride interferences such as $\text{H}_2^{16}\text{O}^-$. Under these conditions, average count rates for $^{16}\text{O}^-$ and $^{18}\text{O}^-$ were $\sim 2 \times 10^9$ and $\sim 4 \times 10^6$ cps respectively. Zircons were presputtered for 1 min, and the total integration time per analysis was 5 min. Errors based on counting statistics are 0.1‰ or less in almost all cases (compare to ANU32_1-7@2). The $^{16}\text{O}^-$ and $^{18}\text{O}^-$ signals were corrected for shifts in the baseline of the Faraday cup detector system from intermittent measurements with the primary and electron beams blanked.

[10] Obvious cracks and metamict regions of individual zircon grains were avoided during analysis, but postanalysis inspection by reflected light (RL), backscatter electron (BSE) or cathodoluminescence imaging (CL) was used to scrutinize (and in some cases exclude from further consideration) problematic analysis spots [e.g., *Cavosie et al.*, 2005]. Cracks and defect structures in zircons are well-known conduits for contaminants [e.g., *Peck et al.*, 2001]. They may act as gateways for diffusive exchange and it is not inconceivable that mount media may seep into microcracks. To explore for oxygen isotope trends in variably altered samples, zircons with variable degrees of Pb-loss (quantified by U-Pb discordance) were analyzed. Exact protocols varied from mount-to-mount ($n = 12$) and these can be classified into three groups.

[11] 1. Sample mount ANU29 was analyzed for oxygen isotopes without prior removal of existing geochronology spots by repolishing. This was done so that analysis spots for in situ oxygen isotopes could be placed adjacent to geochronology spots without overlap. One possible objection to this approach is that the oxygen beam from the duoplasmatron source embeds ^{16}O into zircon regions that may result in anomalously low $\delta^{18}\text{O}$ values [Benninghoven et al., 1987]. We note, however, that this is an extremely local effect (<30 μm) and

it was considered of sufficient benefit to analyze a sample mount in this manner.

[12] 2. Zircons in sample mount JH992CU11 were rapidly characterized for $^{207}\text{Pb}/^{206}\text{Pb}$ ages in “survey mode” following our usual techniques [Mojzsis et al., 2001; Turner et al., 2004; Harrison et al., 2005a]. This procedure was used to identify potentially ancient grains (>3.8 Ga) in a fraction of the time required for a full 10 cycle U-Pb geochronology analysis (~ 10 min). Subsequently, JH992CU11 was repolished with 0.05 μm alumina paste which resulted in the complete removal of all prior ion microprobe pits, cleaned in 1N HCl and DI water baths, Au-coated and measured for oxygen isotopes. After oxygen isotope determinations, U-Pb ion microprobe geochronology analyses were performed precisely in the same place as oxygen isotope measurements.

[13] 3. For all other samples analyzed in this study, zircons were characterized in survey mode, followed by U-Pb geochronology as in (1), except a hand polish followed age determination to remove any trace of preexisting ion microprobe geochronology spots before measurement for oxygen isotopes.

[14] Instrumental mass fractionation (Δ_{imf}), the difference between the actual $^{18}\text{O}/^{16}\text{O}$ of standard grains and that measured by secondary ion mass spectrometry, varied from 1 to 2 per mil (‰). Some of these Δ_{imf} variations are probably associated with slight changes in the geometry of the sample mount after exchange from the sample chamber. To monitor this effect, we collected standard data for each sample mount. Because Δ_{imf} is sensitive to secondary ion generation and extraction conditions related to the geometry of individual mounts, it is crucial to have standard materials cast with the unknowns on the same sample mount. Duluth gabbro zircon AS-3 [Paces and Miller, 1993] is a widely used and abundant geochronology standard [e.g., Schmitz et al., 2003] and has also been used for SIMS oxygen isotope calibration [Booth et al., 2005]. The AS-3 zircon is routinely included on all of our sample mounts. Our standardization protocol calls for an average of 10 individual standard measurements per mount, leading to an average external precision of $\pm 0.7\%$, and in most cases measurements were performed on more than one AS-3 grain per mount (auxiliary material Tables S1 and S2).¹ Overall, standards measurements comprised $>60\%$ of all analyses performed.

¹Auxiliary material data sets are available at <ftp://ftp.agu.org/apend/gc/2006gc001449>. Other auxiliary material files are in the HTML.

330 [15] To evaluate whether Δ_{imf} tracks with compositional variations as “matrix effects” in zircon, we intermittently measured standards KIM-5 ($\delta^{18}\text{O} = +5.09\text{‰}$ [Valley, 2003]) and 91500 ($\delta^{18}\text{O} = +9.86\text{‰}$ [Wiedenbeck et al., 2004]) with AS-3 (+5.34‰; see section 2.2) cast together on a separate standard mount. Matrix effects in oxygen isotopes were not observed within the analytic precision of the ion microprobe for three different standard zircons with HfO_2 values of 0.695 wt.% (91500 [Wiedenbeck et al., 2004]), 1.20 wt.% (AS-3 [Black et al., 2004]), and 1.23 wt.% (KIM-5 [Valley et al., 2003]). The HfO_2 abundance in our primary zircon standard (AS-3) is similar to JH and MN zircon compositions [Cavosie et al., 2005; Maas et al., 1992; Crowley et al., 2005]. Nemchin et al. [2006b] applied Hf-related matrix effects corrections which were originally derived for high-energy-offset analyses [Peck et al., 2001], in contrast to their low-energy-offsets. In the absence of observable matrix effects on our zircon standards, we applied no additional matrix effects corrections to the data.

352 [16] In reflected and transmitted light microscopy, it was apparent that some AS-3 standard grains mounted with the unknowns host inclusions and crack ingrowths of secondary phases such as Fe-oxide. However, secondary features are readily identifiable in optical images used to create maps of the sample mounts, and are easily avoided during analysis. Hence we found no reason to reject any standard analyses.

360 [17] Internal and external analysis errors are reported for unknowns, the latter propagating the variability of the AS-3 standard measurements for each mount. Detector background subtraction for ^{18}O was made by interpolation of bracketed background measurements with the time-stamp of each analysis for standards and unknowns. Corrections for background on ^{16}O were deemed unnecessary due to high count rates ($\sim 10^9$ cps) for zircon analyses relative to background fluctuations ($\sim 10^3$ cps). For each analytical session (reported in Table S1), we calculated the weighted mean of the standard $^{18}\text{O}/^{16}\text{O}$ ratios (Table S2). The final zircon $\delta^{18}\text{O}_{\text{VSMOW}}$ was calculated according to the relation:

$$\delta^{18}\text{O}_{\text{VSMOW}}(\text{zircon}) = \left[\frac{(^{18}\text{O}/^{16}\text{O})_{\text{unkwn}}}{(^{18}\text{O}/^{16}\text{O})_{\text{STD}_{\text{meas}}}/(^{18}\text{O}/^{16}\text{O})_{\text{STD}_{\text{true}}}} - \text{VSMOW} \right] \cdot \frac{1000}{\text{VSMOW}} \quad (1)$$

375 where $^{18}\text{O}/^{16}\text{O}_{\text{unkwn}}$ is the measured unknown background corrected ratio, $^{18}\text{O}/^{16}\text{O}_{\text{STD}_{\text{meas}}}$ is the average measured standard value on a given

Table 1. Laser Fluorination Analyses of Oxygen Isotope Ratios of AS-3 Zircon

	wt, mg	$\delta^{17}\text{O}$	$\delta^{18}\text{O}$	$\Delta^{17}\text{O}$	
Aliquot 1	0.58	2.801	5.368	0.010	t1.3
Aliquot 2	0.65	2.762	5.319	-0.004	t1.4
		$\delta^{18}\text{O}_{\text{ave}} =$	5.344 ± 0.035		t1.5

mount (Table S1), $^{18}\text{O}/^{16}\text{O}_{\text{STD}_{\text{true}}}$ is the true value of the standard (AS-3 = 0.0020159) and VSMOW = 0.0020052.

[18] As a follow-up to the unusually high $\delta^{18}\text{O}$ zircon values previously reported for grain JH992_42 (core = +10‰, rim = +15‰) by Mojzsis et al. [2001], and as a means to simultaneously test for volume homogeneity in oxygen isotopes and agreement between our results and that of earlier studies, this zircon was removed from its original mount with an unpolished prism face placed face down in adhesive tape and recast with AS-3, KIM-5, and 91500. Results of this analysis are presented in section 3.

2.2. Laser-Fluorination Oxygen Isotope Analyses of Standard Zircon AS-3

[19] To prepare zircon standard AS-3 for oxygen isotopic analysis via laser fluorination, we hand-picked ~ 200 inclusion-free grains, separated by standard heavy-mineral techniques from a fresh sample of the original Duluth gabbro. This was done with the view that optically “pure” whole grains are probably reasonable approximations to visibly homogenous regions of the polished AS-3 surfaces chosen for analysis by ion microprobe. Splits of AS-3 were separated into 0.58 and 0.65 mg aliquots and fluorinated by infrared laser heating. Oxygen isotope ratios were analyzed with a Finnigan MAT 252 gas ratio mass spectrometer (UCLA) and absolute $\delta^{18}\text{O}$ zircon values were calibrated against the San Carlos olivine silicate standard (+5.3‰) and globally homogeneous tropospheric O_2 [e.g., Young et al., 1998]. Results in Table 1 use the average $\delta^{18}\text{O}$ value of $+5.34 \pm 0.03\text{‰}$ (1σ) for standard AS-3. Our data are in excellent agreement with separate $\delta^{18}\text{O}$ zircon laser fluorination results on Duluth gabbro zircons ($+5.21 \pm 0.34\text{‰}$) reported by Booth et al. [2005].

2.3. Ti-in-Zircon Concentrations

[20] Titanium concentrations in zircon were measured using the same protocol as Watson et al.

t2.1 **Table 2.** Ion Microprobe Analyses of Oxygen Isotope Ratios of Jack Hills and Mt. Narryer Zircons

t2.2	Grain and Spot	$^{207}\text{Pb}/^{206}\text{Pb}$ Age, Ma	% Concord	Measured $^{18}\text{O}/^{16}\text{O}$	1σ (Internal)	Background Corrected $^{18}\text{O}/^{16}\text{O}$	$\delta^{18}\text{O}_{\text{CALC}}$	1σ (External)	Correlative to Age?
t2.3	ANU29 ^a								
t2.4	1-15@1	4036	94	0.0020251	± 1.40E-07	0.0020235	6.7	± 0.9	y
t2.5	1-15@2			0.0020245	± 1.50E-07	0.0020228	6.4	± 0.9	n
t2.6	11-7@1	3979	95	0.0020262	± 2.00E-07	0.0020247	7.3	± 0.9	n
t2.7	11-9@2	3860	97	0.0020235	± 1.60E-07	0.0020219	5.9	± 0.9	n
t2.8	11-10@1	4012	96	0.0020269	± 1.70E-07	0.0020254	7.7	± 0.9	n
t2.9	12-4@1	4020	98	0.0020253	± 1.50E-07	0.0020238	6.9	± 0.9	y
t2.10	13-11@1	4142	105	0.0020229	± 2.40E-07	0.0020214	5.7	± 0.9	y
t2.11	ANU30								
t2.12	9-1@1	4340	94	0.0020193	± 3.40E-07	0.0020181	5.1	± 0.8	y
t2.13	9-1@2			0.0020200	± 1.40E-07	0.0020186	6.9	± 0.7	n
t2.14	ANU31								
t2.15	1-14@1	4034	96	0.0020207	± 2.54E-07	0.0020200	5.1	± 0.9	y
t2.16	3-11@1			0.0020174	± 1.50E-07	0.0020156	5.2	± 0.2	n
t2.17	3-11@2	3947	95	0.0020192	± 1.60E-07	0.0020173	6.1	± 0.2	y
t2.18	4-10@1	4118	93	0.0020206	± 1.70E-07	0.0020198	5.0	± 0.9	y
t2.19	4-14@1	4121	93	0.0020194	± 1.00E-07	0.0020185	4.4	± 0.9	y
t2.20	5-1@1	4058	94	0.0020193	± 2.80E-07	0.0020186	4.4	± 0.9	y
t2.21	7-5@1	3981	95	0.0020207	± 1.70E-07	0.0020200	5.1	± 0.9	y
t2.22	8-4@1	4111	94	0.0020198	± 1.90E-07	0.0020190	4.6	± 0.9	y
t2.23	10-11@1	4040	93	0.0020196	± 2.10E-07	0.0020189	4.6	± 0.9	y
t2.24	12-12@1	4064	93	0.0020214	± 2.10E-07	0.0020207	5.5	± 0.9	y
t2.25	14-3@1	4121	95	0.0020223	± 2.00E-07	0.0020216	5.9	± 0.9	y
t2.26	14-7@1	4127	93	0.0020229	± 2.20E-07	0.0020221	6.2	± 0.9	y
t2.27	15-8@1	4111	95	0.0020216	± 1.30E-07	0.0020208	5.5	± 0.9	y
t2.28	ANU32								
t2.29	1-7@1	4021	92	0.0020182	± 2.10E-07	0.0020170	5.5	± 0.6	y
t2.30	1-7@2			0.0020283	± 1.60E-06	0.0020269	10.5	± 0.8 ^b	n
t2.31	2-15@1	4012	93	0.0020190	± 1.80E-07	0.0020179	5.9	± 0.6	y
t2.32	2-15@2			0.0020199	± 1.30E-07	0.0020188	6.4	± 0.6	n
t2.33	6-9@1	4070	95	0.0020185	± 1.40E-07	0.0020174	5.7	± 0.6	y
t2.34	6-10@1			0.0020189	± 1.40E-07	0.0020178	5.9	± 0.6	y
t2.35	6-10@2	4152	91	0.0020194	± 1.50E-07	0.0020183	6.1	± 0.6	y
t2.36	6-15@1	4092	92	0.0020189	± 1.20E-07	0.0020178	5.9	± 0.6	y
t2.37	6-15@2			0.0020208	± 1.80E-07	0.0020197	6.8	± 0.6	y
t2.38	8-13@1	3993	94	0.0020184	± 1.60E-07	0.0020174	5.7	± 0.6	y
t2.39	11-5@1	4068	94	0.0020130	± 1.80E-07	0.0020118	2.9	± 0.6	y
t2.40	11-5@2			0.0020196	± 1.40E-07	0.0020186	6.3	± 0.6	y
t2.41	ANU33								
t2.42	1-4@1	3995	92	0.0020200	± 1.50E-07	0.0020186	5.6	± 0.8	y
t2.43	5-2@1	3929	97	0.0020194	± 1.40E-07	0.0020181	5.3	± 0.8	y
t2.44	5-3@1	4054	95	0.0020194	± 1.30E-07	0.0020181	5.3	± 0.8	y
t2.45	6-14@1	4065	91	0.0020227	± 1.80E-07	0.0020212	6.8	± 0.8	n
t2.46	7-3@1	3994	96	0.0020200	± 1.50E-07	0.0020186	5.6	± 0.8	y
t2.47	7-15@1	4004	98	0.0020215	± 1.60E-07	0.0020200	6.2	± 0.8	y
t2.48	8-1@1	3995	93	0.0020191	± 1.70E-07	0.0020178	5.1	± 0.8	y
t2.49	8-1@2			0.0020207	± 1.50E-07	0.0020194	6.0	± 0.8	n
t2.50	11-15@1			0.0020230	± 1.50E-07	0.0020215	7.0	± 0.8	n
t2.51	11-15@2	4117	96	0.0020210	± 1.80E-07	0.0020196	6.0	± 0.8	y
t2.52	12-7@1	3903	97	0.0020218	± 1.50E-07	0.0020204	6.5	± 0.8	y
t2.53	12-14@1	4001	97	0.0020221	± 1.30E-07	0.0020206	6.6	± 0.8	y
t2.54	12-14@2			0.0020240	± 1.30E-07	0.0020226	7.5	± 0.8	n
t2.55	13-6@1	4063	92	0.0020205	± 1.40E-07	0.0020191	5.8	± 0.8	y
t2.56	14-9@1	4084	95	0.0020213	± 1.40E-07	0.0020199	6.2	± 0.8	y
t2.57	15-11@1	4196	96	0.0020218	± 1.50E-07	0.0020204	6.4	± 0.8	y
t2.58	15-11@2			0.0020231	± 1.40E-07	0.0020217	7.1	± 0.8	n
t2.59	JH0101-1								
t2.60	6-10@1	3919	94	0.0020179	± 1.60E-07	0.0020170	5.8	± 1.0	y
t2.61	9-18@2	3811	98	0.0020181	± 1.30E-07	0.0020153	5.0	± 1.0	y
t2.62	9-20@1	3925	92	0.0020141	± 1.20E-07	0.0020131	3.9	± 1.0	y

Table 2. (continued)

	$^{207}\text{Pb}/^{206}\text{Pb}$	%	Measured	1σ	Background	$\delta^{18}\text{O}_{\text{CALC}}$	1σ	Correlative	
t2.63	Grain and Spot	Age, Ma	Concord	$^{18}\text{O}/^{16}\text{O}$	(Internal)	Corrected $^{18}\text{O}/^{16}\text{O}$	(External)	to Age?	
t2.64	9-20@3			0.0020137 ±	1.10E-07	0.0020126	3.6 ±	n	
t2.65	10-4@1	3852	95	0.0020183 ±	1.90E-07	0.0020172	5.9 ±	y	
t2.66	JH0101-CC01								
t2.67	2-3@3	4091	100	0.0020175 ±	1.60E-07	0.0020162	5.0 ±	y	
t2.68	2-3@4			0.0020186 ±	9.70E-08	0.0020174	5.6 ±	y	
t2.69	JH0101-2								
t2.70	3-15@1	4230	99	0.0020207 ±	1.10E-07	0.0020191	5.7 ±	y	
t2.71	7-18@1	4091	99	0.0020193 ±	1.40E-07	0.0020176	4.9 ±	y	
t2.72	10-17@1	4074	100	0.0020188 ±	1.10E-07	0.0020174	4.8 ±	y	
t2.73	10-17@2			0.0020171 ±	1.30E-07	0.0020157	3.9 ±	n	
t2.75		<i>MN0102-1 (grains located in matrix) collected from Mount Narryer</i>							
t2.76	1-1@1	4042	99	0.0020132 ±	1.20E-07	0.0020119	5.5 ±	y	
t2.77	2-7@1	4137	103	0.0020125 ±	1.50E-07	0.0020112	5.1 ±	y	
t2.78	2-7@2	4113	97	0.0020133 ±	1.30E-07	0.0020119	5.5 ±	y	
t2.79	JH992CU11 ^c								
t2.80	2-10@2	3863	107	0.0020225 ±	1.29E-07	0.0020221	6.8 ±	y	
t2.81	4-8@1	4083	99	0.0020211 ±	1.30E-07	0.0020206	6.1 ±	y	
t2.82	4-8@2	4076	105	0.0020203 ±	1.60E-07	0.0020198	5.7 ±	y	
t2.83	4-9@2	4017	101	0.0020205 ±	9.10E-08	0.0020200	5.8 ±	y	
t2.84	6-10@1	4110	99	0.0020201 ±	1.10E-07	0.0020195	5.5 ±	y	
t2.85	8-6@1	4126	94	0.0020208 ±	1.90E-07	0.0020202	5.8 ±	y	
t2.86	8-6@2	4133	94	0.0020200 ±	9.80E-08	0.0020194	5.5 ±	y	

t2.87 ^aSample unpolished prior to oxygen isotope analyses.

t2.88 ^bInternal error is greater than external error.

t2.89 ^cOxygen work performed prior to geochronology.

421 [2006]; a brief summary is provided. Data for
 422 $[\text{Ti}]_{\text{zircon}}$ were collected with a CAMECA ims 3f
 423 ion microprobe at Woods Hole Oceanographic
 424 Institution. Duplicate measurements on pre-4.0 Ga
 425 zircons for two mounts (JH0101-2 and JH992-
 426 CU11) were made at different grain locations. A
 427 primary 5 nA O^- beam was focused to a 15–20 μm
 428 spot on synthetic zircon standards of known Ti
 429 concentrations as determined by electron micro-
 430 probe. Synthetic zircons grown at high temper-
 431 atures ($\sim 1400^\circ\text{C}$) and characterized for their Ti
 432 concentrations by electron microprobe were used
 433 with natural samples as ion microprobe standards.
 434 The combined electron and ion microprobe analyt-
 435 ical uncertainty for zircons crystallizing in the 650–
 436 700°C range relevant to this study is $\sim 5^\circ\text{C}$ (1σ).
 437 Minimum detection limits for Ti by this method are
 438 ~ 0.1 ppm. The measured concentrations applied to
 439 the equation define a log linear dependence of Ti
 440 with temperature as presented by *Watson et al.*
 441 [2006]. The uncertainties on the constants of the
 442 thermometry equation propagate an error of $\sim 5^\circ\text{C}$
 443 (1σ) for temperatures reported here. When it was
 444 possible to do so, cracks were avoided because it
 445 has been found that measured Ti concentrations are
 446 often elevated when analyses occur on cracks in

zircon [*Watson and Harrison, 2005; Watson et al.,* 447
 2006]. 448

3. Results 450

3.1. Hadean Zircon Oxygen Isotopes and CL Imagery 451

[21] We analyzed 89 JH and MN zircons with a 453
 total of 139 separate oxygen spots; many measure- 454
 ments can be directly correlated with the locations 455
 of previously documented U-Pb geochronological 456
 analyses. The 72 spot data identified as analytically 457
 reliable on the basis of the absence of cracks and 458
 inclusions at the measurement location are reported 459
 in Table 2. These data comprise measured pre- 460
 background-corrected and post-background- 461
 corrected $^{18}\text{O}/^{16}\text{O}$ ratios, zircon $\delta^{18}\text{O}$ for the 462
 unknowns and results for $\leq 10\%$ discordant geo- 463
 chronology spots collected in the vicinity of the 464
 oxygen spots. All O-isotope measurements made 465
 during our four day ion microprobe session (with 466
 standards and data subsequently rejected on the 467
 basis of the criteria outlined above) are reported in 468
 auxiliary material Table S2. Sample data for anal- 469
 yses on grain cracks, $<90\%$ concordant zircons, 470
 and/or grains younger than 3800 Ma are tabulated 471

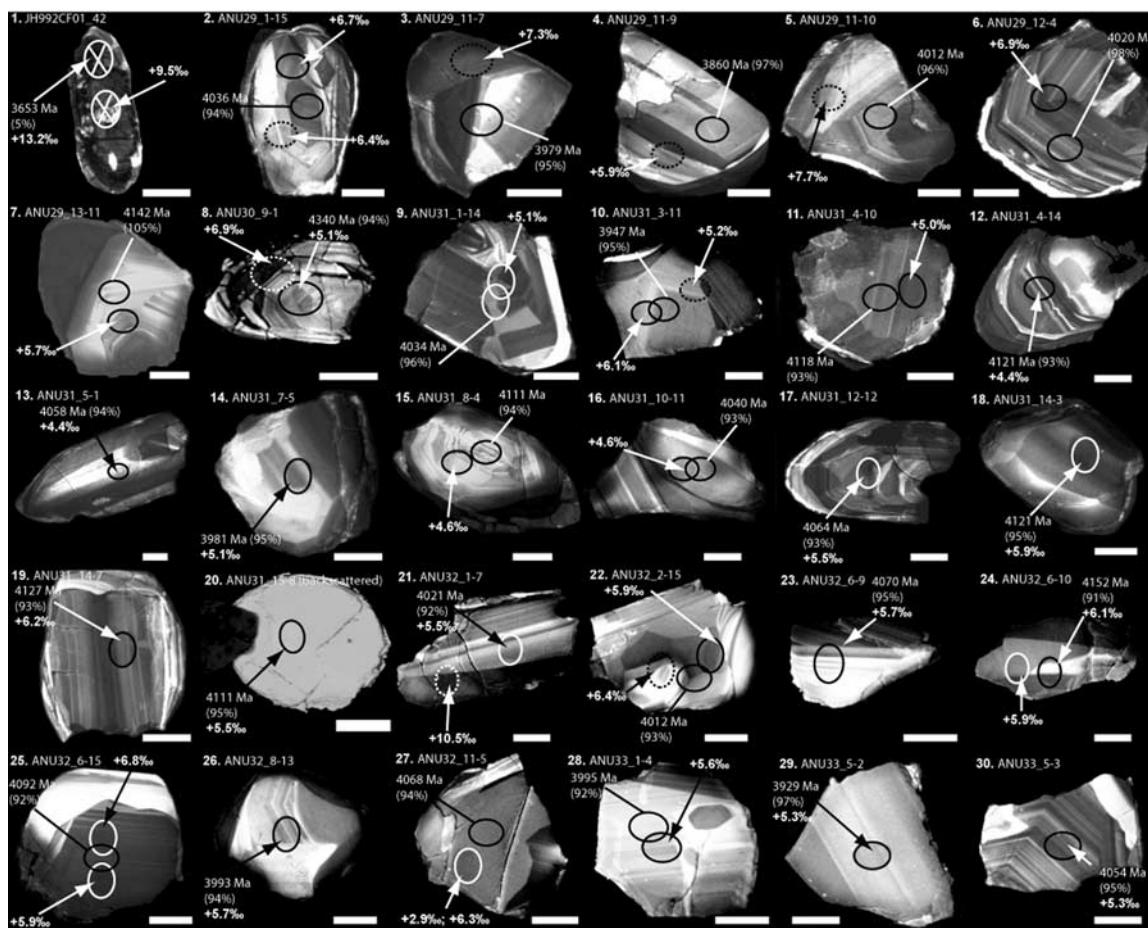


Figure 1. Cathodoluminescence images of zircons in Table 2 with geochronology and oxygen data. Ion microprobe spots with an “X” represent an analysis on a crack or on a discordant grain region, and dashed ion microprobe spots represent an analysis free of analytical artifacts, but which cannot be correlated with age. All zircons contain at least 1 geochronology spot >90% concordant except for JH992_42, which is shown as a follow-up and a confirmation of previous work [Mojzsis *et al.*, 2001]. Grain ANU31_15-8 was inadvertently not imaged in CL. Boxed images contain Ti temperature measurements (section 3.3).

472 separately in auxiliary material Table S3. Catho-
473 doluminescence images for Hadean grains which
474 were analyzed on cracks grains can be found in
475 Figure S1. Data free of analytical artifacts (Table 2)
476 display a peak in $\delta^{18}\text{O}$ at +5.8‰ that is similar to
477 the average of 28 analysis spots on eight pre-4.2 Ga
478 zircons reported by *Nemchin et al.* [2006a], and
479 lower by $\sim 0.4\text{‰}$ when compared to the 41 zircons
480 standardized with KIM-5 from *Cavosie et al.*
481 [2005]. The reason for the difference between our
482 results and *Cavosie et al.* [2005] may be due to
483 $\delta^{18}\text{O}$ zircon heterogeneity among samples, but
484 analytical bias due to different procedures in the
485 oxygen standardization (or the standard itself)
486 cannot be excluded.

487 [22] In order to assess whether these differences in
488 oxygen isotope values are statistically significant,
489 we have used the Kolmogorov-Smirnov (K-S) test

to compare zircon $\delta^{18}\text{O}$ values of individual studies. 490
The K-S test has been widely used in Earth 491
Sciences [e.g., *Miller and Kahn*, 1962], and is 492
advantageous because unlike the “t-test” it is 493
distribution free. In our analysis, we used the 494
Gaussian kernel probability function described by 495
Silverman [1986]. In addition, our comparison 496
takes into consideration the external error for each 497
zircon. Results indicate that data from Table 2 and 498
Nemchin et al. [2006a] fulfill the requirements of a 499
single population of oxygen isotope values in the 500
Hadean zircons at the 95% confidence level. How- 501
ever, when our data are compared to the data set of 502
Cavosie et al. [2005], the probability that the 503
zircons were derived from the same population is 504
<5%. Despite these differences, our results validate 505
previous findings that Hadean zircons on average 506
are enriched above mantle equilibrium values. 507

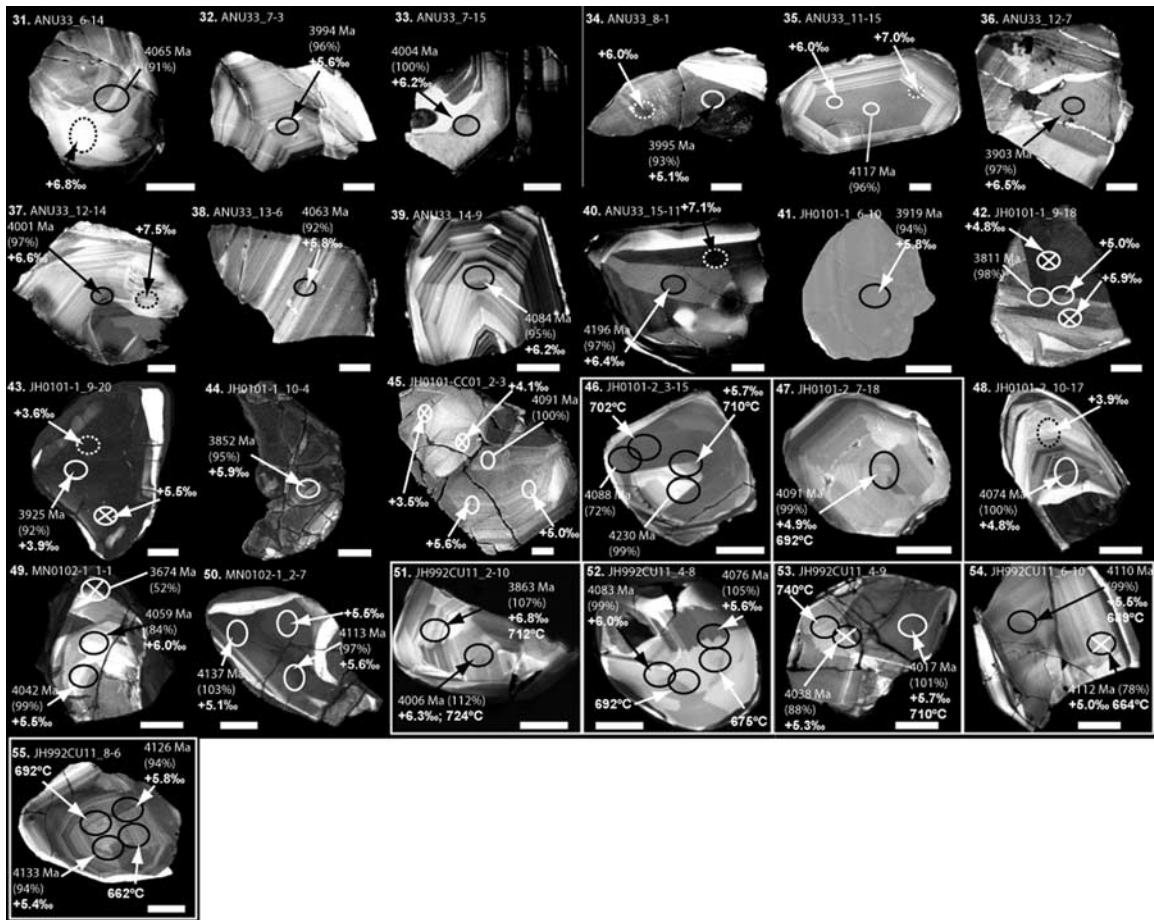


Figure 1. (continued)

508 [23] For two of our zircon grains, the Cs-ion beam
509 used for oxygen isotope measurements overlapped
510 unpolished geochronology spots (ANU29_11–9:
511 Figure 1, no. 4; ANU29_10–6: Figure S1, no. 64).
512 As expected, the measured $\delta^{18}\text{O}$ values are +2.0‰
513 and +2.3‰, respectively, which reflects ^{16}O
514 contamination from the $^{16}\text{O}_2^-$ ion beam [Benninghoven
515 *et al.*, 1987]. The block data of these two analyses
516 show the expected systematic increase in $^{18}\text{O}/^{16}\text{O}$
517 with depth as the contaminant ^{16}O decreases. Such
518 increase is not seen in other measured unknowns
519 where beam spot overlap was avoided, which means
520 that the influence of implanted ^{16}O is negligible
521 outside of the exact locality of the previous analysis
522 spot.

523 [24] Figure 1 shows CL images labeled with geo-
524 chronology and oxygen results and analysis spot
525 locations. While some zircons show interpretable
526 core-rim relationships in CL (e.g., Figure 1: no. 2,
527 6–8, 12, 15, 17, 25, 39, 48, 51, 55), such patterns
528 are diffuse in other cases (e.g., Figure 1: no. 16, 18,
529 21, 22, 27, 29, 30, 38) and a core/rim assignment to

individual spots is ambiguous in many crystals. In
530 light of this observation, Table 2 reports whether
531 the oxygen spot locations can be correlated to
532 geochronology spots on the basis of CL patterns.
533 For example, in Figure 1, no. 35, the geochronology
534 spot and the +6.0‰ oxygen measurement were not
535 made on top of one another, but the similarity of
536 CL patterns supports the interpretation that the two
537 are part of the same grain domain. Zircons outlined
538 by white boxes in Figure 1 were further investi-
539 gated for Ti thermometry (section 3.3). Data from
540 50 zircons in Table 2 from 57 ion microprobe
541 oxygen spots from this data set can be directly
542 correlated with U-Pb geochronology. Some zircons
543 were analyzed so that both geochronology and
544 O-isotopes were collected in the same grain do-
545 main after polishing. For analyses where correlated
546 $^{207}\text{Pb}/^{206}\text{Pb}$ ages can be established, 15 (~25%)
547 yield $\delta^{18}\text{O}$ values greater than or equal to 6.0‰
548 and 5 (~10%) yield values $\geq 6.5‰$.
549

[25] In Figure 2, two distributions for $\delta^{18}\text{O}$ values
550 in zircons ≥ 3.8 Ga are plotted: (1) $\geq 90\%$ concor-
551

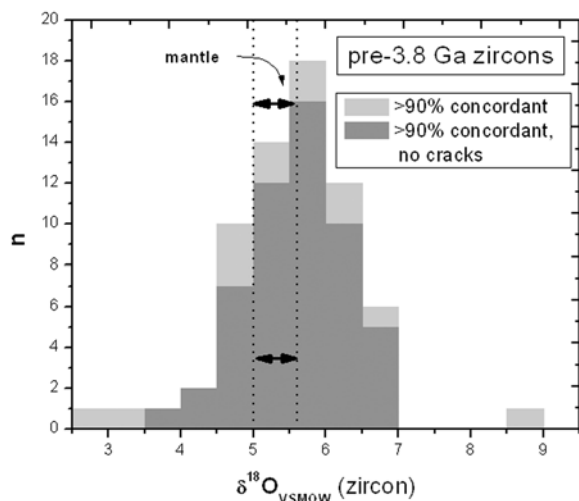


Figure 2. Frequency distribution of $\delta^{18}\text{O}_{\text{VSMOW}}$ (zircon) measurements of pre-3.8 Ga grains. The distribution is divided into two categories: (1) all zircons measured with a correlative age spot which are at least 90% concordant and (2) all zircons which fall under category 1, but where the $\delta^{18}\text{O}$ analysis spot is not located on a grain crack based on detailed retrospective imaging studies. We find that the average oxygen isotopic composition derived for analyses performed on zircons where cracks are present and those without are within 0.1‰ of each other, but the range of $\delta^{18}\text{O}$ of grains with cracks is greater.

552 dant and (2) $\geq 90\%$ concordant without cracks on or
553 near oxygen analysis spots. The lowest $\delta^{18}\text{O}$ zircon
554 value obtained in our analysis was +2.9‰ (Table 2:
555 ANU32_11-5; Figure 1; no. 27); however, a succes-
556 sive measurement of the same spot recorded a value
557 of +6.3‰. The two highest values we obtained were
558 +10.5‰ (not plotted) measured on a region of grain
559 ANU32_1-7 of uncertain age (Table 2: ANU32_1-7;
560 Figure 1; no. 21) and +8.6‰ on a concordant but
561 cracked grain region (Table S3: JH992CU11_8-6;
562 Figure S1: no. 84).

563 [26] Our remeasurement of JH992_42 (reported by
564 *Mojzsis et al.* [2001]; Figure 1, no. 1) mounted
565 with AS-3, 91500, and KIM-5 yielded zircon core
566 and rim values that vary slightly with the standard
567 used for instrumental mass fractionation correction:
568 9.5‰/13.2‰ (AS-3; 1 s.e. = $\pm 0.6\%$), 9.7‰/13.4‰
569 (91500; 1 s.e. $\pm 1.4\%$), and 8.9‰/12.6‰ (KIM-5;
570 1 s.e. $\pm 0.3\%$). The differences in $\delta^{18}\text{O}$ zircon
571 instrumental mass fractionation corrections using
572 different standards (all measured on the same
573 mount) are small and agree within error. Because
574 data collected here were taken from an opposite
575 prism face of JH992_42, we find the results
576 in good agreement with the core/rim values of

+10‰/ + 15‰ from *Mojzsis et al.* [2001]. How- 577
ever, because this zircon is highly discordant 578
[*Mojzsis et al.*, 2001], we deem it unlikely that 579
this zircon records primary $\delta^{18}\text{O}$ values. 580

3.2. Oxygen Isotope Systematics in Variably 582 Discordant Zircons 583

[27] To explore for possible zircon oxygen isotope 584
correlations, we analyzed a suite of variably discor- 585
dant Jack Hills zircons, which most likely become 586
discordant at low temperatures. Uranium-lead con- 587
cordance % versus $\delta^{18}\text{O}_{\text{VSMOW}}$ zircon data (Table 1 588
and Table S3) and results from *Cavosie et al.* [2005] 589
are plotted in Figure 3. These data also incorporate 590
some grains that are < 3.8 Ga (Table S3). Data were 591
divided into three categories: (1) $\delta^{18}\text{O}$ zircon mea- 592
surements interpreted as magmatic with correlative 593

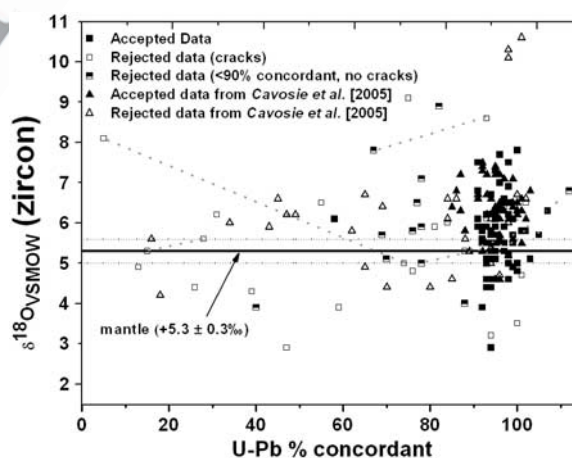


Figure 3. Comparison of zircon $\delta^{18}\text{O}_{\text{VSMOW}}$ versus U/Pb concordance (%) where correlative $\delta^{18}\text{O}$ and geochronology measurements are documented. In this study, zircons with multiple $\delta^{18}\text{O}$ versus age spots are connected by (dashed) tie lines. This plot also includes some grains younger than 3800 Ma and reported in Table S3 which are not present in Figure 2. Results have been divided into three categories: (1) analyses on a grain crack (open symbol), (2) analyses on zones greater than 10% discordant (semi-open symbol), and (3) analyses do not meet categories 1 and 2, and are most likely to represent the $\delta^{18}\text{O}$ of primary crystallization (closed symbol). Also included in this figure are data from *Cavosie et al.* [2005]. We find that zircons which are more discordant appear to have lower (measured) $\delta^{18}\text{O}$ values. The two exceptions are JH992CU11_10-8 and JH992_42, which record values of +8.1‰ and +13.2‰ (off scale), respectively, and both are 5% concordant. This result may be symptomatic of oxygen exchange with the homogenous Jack Hills sediments, where $\delta^{18}\text{O}$ values $\geq 10\%$ have been reported [*Cavosie et al.*, 2005].

t3.1 **Table 3.** Ion Microprobe Analyses of Ti Concentrations of Jack Hills Zircons

t3.2	Grain and Spot	$^{49}\text{Ti}/^{30}\text{Si}$	ppm Ti	T, °C
t3.3	JH0101-2			
t3.4	3-15a	0.000115	7	710
t3.5	3-15b	0.000104	6.3	702
t3.6	5-11a	0.000022	1.3	588
t3.7	5-11b	0.000039	2.4	629
t3.8	5-11c	0.000038	2.3	626
t3.9	7-18	0.000092	5.6	692
t3.10	8-8	0.000049	3	645
t3.11	8-10	0.00011	6.7	707
t3.12	9-15a	0.000041	2.5	632
t3.13	9-15b	0.000353	21.4	812 ^a
t3.14	9-15c	0.000139	8.4	726
t3.15	JH992-CU11			
t3.16	1-7a	0.000105	6.4	703
t3.17	1-7b	0.000084	5.1	685
t3.18	2-10a	0.000118	7.1	712
t3.19	2-10b	0.000135	8.2	724
t3.20	3-7a	0.000682	41.3	883 ^a
t3.21	3-7b	0.001932	116.9	1015 ^a
t3.22	4-8a	0.000092	5.6	692
t3.23	4-8b	0.000075	4.5	675
t3.24	4-9a	0.000116	7	710
t3.25	4-9b	0.000163	9.9	740
t3.26	6-10a	0.000089	5.4	689
t3.27	6-10b	0.000064	3.9	664
t3.28	8-6a	0.000092	5.6	692
t3.29	8-6b	0.000062	3.8	662

t3.30 ^aLarge cracks present on analytical surface.

594 geochronology; (2) oxygen data (regardless of
595 concordance) where retrospective image studies
596 revealed oxygen measurements were collected on
597 grain cracks; and (3) data which do not overlap
598 cracks, but are from zircon domains $\geq 10\%$ discordant.
599 The figure shows that more discordant zircons
600 do not tend toward the isotopically heavy O-isotope
601 composition ($\delta^{18}\text{O} \geq +10\%$) of the host quartz-
602 pebble conglomerates at the Jack Hills [Cavosie
603 *et al.*, 2005].

604 [28] The data are not entirely systematic; zircon
605 $\delta^{18}\text{O}$ values for two highly discordant grains
606 (JH992CU11_10-8: Figure S1, no. 89; JH992_42:
607 Figure 1, no. 1) deviate from this trend and one of
608 these (JH992CU11_10-8) hosts a visibly metamict
609 domain. This behavior in $\delta^{18}\text{O}$ zircon versus U/Pb
610 concordance % has also been observed for mea-
611 surements of whole zircon splits, where more
612 discordant aliquots tend to have lower $\delta^{18}\text{O}$ values
613 [Bibikova *et al.*, 1982; Valley *et al.*, 1994]. A
614 separate study analyzed grains by ion microprobe
615 and reported a similar trend toward lower $\delta^{18}\text{O}$
616 values in zircons with decreasing U/Pb concor-
617 dance at the scale of tens of micrometers [Booth
618 *et al.*, 2005].

3.3. Jack Hills Zircon Ti Thermometry

620

[29] Table 3 reports zircon Ti concentrations
621 and corresponding crystallization temperatures for
622 13 grains; the 25 spot locations are shown in
623 Figure 1 and Figure S1. These results record an
624 average value of 682°C which agrees well with
625 previous Hadean zircon measurements [Watson
626 and Harrison, 2005, 2006; Valley *et al.*, 2006].
627 This average excludes three “temperatures” which
628 were the result of contamination in Ti due to large
629 cracks on the analytical surfaces. This observation
630 provides justification for our rationale to reject
631 oxygen analyses taken on visible cracks. Our
632 multiple Ti concentration measurements allow for
633 intragrain temperature comparisons, which are
634 made on the basis of the internal error associated
635 with counting statistics, not the external error
636 associated with reproducibility of the standard
637 [Watson *et al.*, 2006]. Most replicate analyses are
638 indistinguishable within analytical precision of the
639 CAMECA 3f ion microprobe, indicating general Ti
640 homogeneity among individual grains. 641

[30] Grain JH0101-2_5-11 (Figure S1, no. 78;
642 $\sim 40\%$ concordant, 3997 Ma) analyzed in triplicate,
643 records temperatures of 588°C, 626°C, and 629°C,
644 outside the range of internal error and reflects the
645 lowest temperatures yet reported for a JH zircon.
646 The two nearly concordant grains with internal
647 temperature differences are JH992CU11_4-9 and
648 JH992CU11_8-6. Grain JH992CU11_4-9 contains
649 4038 Ga and 4017 Ga geochronology spots correla-
650 tive with 740°C and 710°C temperatures, respec-
651 tively. JH992CU11_8-6 records temperatures of
652 662°C and 692°C. The geochronology spots do
653 not directly overlay these temperature measure-
654 ments, but the 692°C spot corresponds to a grain
655 region slightly closer to the cathodoluminescent
656 center (Figure 1, no. 55). These results may record
657 the cooling history of these Hadean zircons. In
658 other words, a cooling magma still saturated in
659 zircon would be expected to continue to grow
660 zircon, but with a lower Ti content reflecting the
661 cooler melt conditions. Such intragrain temperature
662 variations were also noted by Watson and Harrison
663 [2005]. 664

4. Discussion

666

4.1. Oxygen Isotopes in Hadean Zircon

667

[31] A compilation of age-indexed pre-4.0 Ga
668 zircon oxygen data (Table 2) with our new results
669 is presented in Figure 4 [Mojzsis *et al.*, 2001; Peck
670

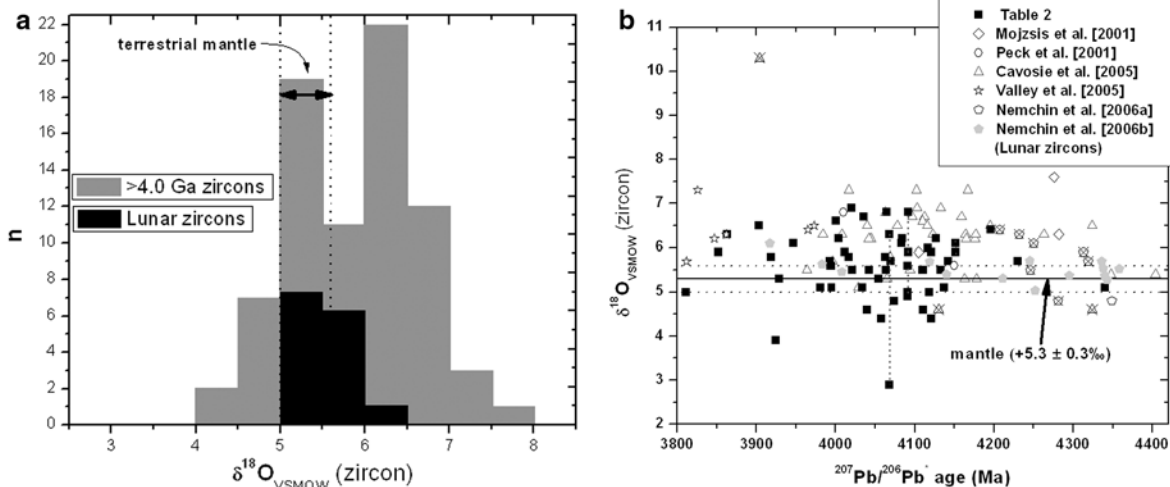


Figure 4. (a) Zircons with ion microprobe U-Pb geochronology ages >4 Ga and correlative $\delta^{18}\text{O}_{\text{VSMOW}}$ (zircon) measurements. The accepted data reported by respective works are as follows: *Mojzsis et al.* [2001] ($n = 3$), *Peck et al.* [2001] ($n = 2$), *Cavosie et al.* [2005] ($n = 33$), *Nemchin et al.* [2006a] ($n = 1$), and data from Table 2 ($n = 38$). Lunar zircon data from *Nemchin et al.* [2006b] in black show that these define a more restricted field of values compared to terrestrial Hadean zircons. (b) Oxygen data plotted versus $^{207}\text{Pb}/^{206}\text{Pb}$ age for Hadean zircons; error bars have been removed for clarity. The data set is as follows: *Mojzsis et al.* [2001] ($n = 3$; $1\sigma = \pm 0.3\%$), *Peck et al.* [2001] ($n = 2$; $1\sigma = \pm 0.8\%$), *Cavosie et al.* [2005] ($n = 37$; $1\sigma = \pm 0.4\%$), *Nemchin et al.* [2006a] ($n = 8$; $1\sigma = \pm 0.3\%$), *Valley et al.* [2005] ($n = 6$; errors not reported), and data from Table 2 ($n = 53$; $1\sigma = \pm 0.7\%$). *Mojzsis et al.* [2001] reported internal errors; all others are reported as external. Primarily, error differences arise from the standard AS-3 (Table 2) versus 91500 [*Nemchin et al.*, 2006a] versus KIM-5 [*Cavosie et al.*, 2005] and the style of analysis, i.e., monocollection [*Peck et al.*, 2001] versus multicollection [e.g., *Mojzsis et al.*, 2001]. Data accepted by Cavosie are 85% concordant or better; data we report here from Table 2 are 90% concordant or better, after analysis of data presented in Figure 3. Crosses through data points are those rejected by *Cavosie et al.* [2005] and *Nemchin et al.* [2006a] on the basis of “non-magmatic zoning” from their analysis of CL images.

671 *et al.*, 2001; *Cavosie et al.*, 2005; *Valley et al.*,
672 2005; *Nemchin et al.*, 2006a] along with lunar
673 data for comparison [*Nemchin et al.*, 2006a]. The
674 compilation includes only those zircon data
675 accepted by various workers on the basis of
676 separately established criteria what constitutes
677 “primary” oxygen isotope values. It is evident
678 from the data in Figure 4a that the terrestrial
679 Hadean zircon oxygen isotope distribution contains
680 a peak offset from mantle zircon by about +1‰
681 and that these values extend well beyond the
682 highest measured lunar zircon oxygen isotopes
683 (Figure 4a). This observation argues against
684 a scenario in which Hadean zircons were exclu-
685 sively derived from protoliths in equilibrium
686 with the mantle, or that they formed in some
687 process that could only have been common to the
688 Earth and Moon. Furthermore, the probability of
689 identical populations viz. Kolmogorov-Smirnov
690 (section 3.1) is <5% for the $\delta^{18}\text{O}$ zircon distribu-
691 tion in Table 2, in comparison with lunar zircon
692 results reported by *Nemchin et al.* [2006b].

[32] Zircon oxygen analyses results considered in 693
equilibrium with the mantle total 26 ($5.3 \pm 0.3\%$), 694
while we find that 24 are above mantle values, 695
and 7 are below +5.0‰. This observation is 696
supported by another Hadean oxygen isotope data 697
set where there is some evidence of oxygen isotope 698
bimodality [*Cavosie et al.*, 2005]. Elevated $\delta^{18}\text{O}$ 699
compositions of Hadean zircons further support the 700
hypothesis that zircon source-melts may have 701
interacted with liquid water at or near Earth’s 702
surface in the Hadean [*Mojzsis et al.*, 2001; *Peck* 703
et al., 2001; *Wilde et al.*, 2001; *Valley et al.*, 2002; 704
Cavosie et al., 2005]. If this interpretation is 705
correct, it is worth exploring whether stable liquid 706
water persisted at Earth’s surface for much or all of 707
the Hadean. This expanded data set coupled 708
with other separate lines of evidence (sections 4.3 709
and 4.5) suggests that some of the Hadean source 710
melt precursors were in chemical communication 711
at or near the surface of the Earth. 712

[33] When all available Hadean $\delta^{18}\text{O}$ zircon 713
results are plotted versus $^{207}\text{Pb}/^{206}\text{Pb}$ zircon age 714
(Figure 4b) it is apparent that data are sparse for 715

716 both the 4.4–4.2 Ga and 3.95–3.85 Ga time
 717 intervals. Hence secular changes in $\delta^{18}\text{O}$ zircon
 718 values from 4.4 Ga to 4150 Ma [Cavosie *et al.*,
 719 2005] need to be verified with more data, but
 720 available records seem to indicate water-rock
 721 interaction (and thus enriched $\delta^{18}\text{O}$ zircon values)
 722 as early as 4.3–4.2 Ga. Progressively more posi-
 723 tive and negative ε_{Hf} values as a function of time in
 724 Hadean zircons have been interpreted to show that
 725 substantial continental crust formation began at
 726 4.4–4.5 Ga [Harrison *et al.*, 2005, 2006; cf. Valley
 727 *et al.*, 2006]. A consequence of the (rapid?) early
 728 increase in the volume of continental crust would
 729 be subsequent increases in the volume of recycled
 730 supracrustal rocks, which in turn led to Hadean
 731 melts that crystallized zircons with more elevated
 732 $^{18}\text{O}/^{16}\text{O}$ values.

733 [34] Is a decrease in $\delta^{18}\text{O}$ zircon values at 3.95 Ga
 734 and after (Figure 4b) preserved? On the basis of the
 735 secular Hf isotopic evolution observed for the
 736 Hadean, Harrison *et al.* [2005] postulated that
 737 massive remixing of Hadean crust back into the
 738 mantle must have occurred because large (± 200) ε_{Hf}
 739 values are not preserved on the contemporary Earth
 740 [Vervoort and Blichert-Toft, 1999]. Under this
 741 scenario, any enriched ^{18}O crust signature would
 742 become diluted when mixed back into the mantle.
 743 Amelin [2005] proposed that the onset of the Late
 744 Heavy Bombardment could have facilitated the
 745 return of crust to the mantle. Again, due to the
 746 relatively small number of 3.95–3.8 Ga zircons
 747 analyzed, more combined oxygen and Hf isotopic
 748 work [Kemp *et al.*, 2006] could either bolster or
 749 refute this model.

750 [35] Two Hadean zircons (JH0101-1_9-20 and
 751 ANU32_11-5) preserved $\delta^{18}\text{O}$ zircon compositions
 752 well below mantle values (Figure 4a). Grain
 753 JH0101-1_9-20 (3925 Ma) has a value of +3.9‰
 754 (Figure 1, no. 43). This zircon shows subdued
 755 CL zoning in its core region, but retains a high-
 756 luminescent rim; all data derived from zircons of
 757 this type were rejected by Cavosie *et al.* [2005]
 758 because they failed to fit their criterion for well-
 759 defined concentric zoning in CL. Two other
 760 (rejected) oxygen spots on the same grain yielded
 761 +3.6‰, and a near-rim value of 5.5‰. Results for
 762 grain ANU32_11-5 are puzzling since two meas-
 763 urements made on top of each other yield very
 764 different oxygen isotope compositions (+2.9‰
 765 versus +6.3‰). One analytical aspect of concern
 766 is the +2.9‰ measurement shows a $\sim 15\%$ de-
 767 crease in ^{16}O and ^{18}O counts relative to other
 768 measurements where signals were generally repro-

ducible to within $\sim 5\%$. In BSE, or reflected light
 images, there is nothing unusual about these grains
 and no cracks or irregularities exist in the vicinity
 of the analysis (Figure 1, no. 27). Minute inclu-
 sions in zircon could impart oxygen heterogeneity,
 but it is also not out of the realm of possibility that
 these zircons record a process in the Hadean crust
 capable of imparting ^{16}O -rich oxygen (relative to
 mantle) to zircon domains. Low and even negative
 $\delta^{18}\text{O}$ whole rock values are sometimes present
 where large meteoric convective hydrothermal sys-
 tems have been established [Taylor and Sheppard,
 1986]. These hydrothermally altered rocks can then
 be remelted to form low $\delta^{18}\text{O}$ magmatic zircons
 [e.g., Bindeman and Valley, 2001].

4.2. Preservation of Primary $\delta^{18}\text{O}$ Values in Hadean Zircons

[36] To evaluate whether measured oxygen isotope
 ratios reflect their crystallization environment
 requires an understanding of oxygen retention in
 zircon, and knowledge of the geologic history of
 Hadean zircons. We review some empirical and
 experimental results for oxygen retention in zircon,
 and discuss the likelihood of primary oxygen
 preservation, given current understanding of pre-
 depositional and postdepositional histories of these
 grains.

[37] Coherent zircon crystal cores, interpreted as
 such from their oscillatory cathodoluminescence
 (CL) patterns, have been interpreted to retain
 original isotope compositions through a variety of
 metamorphic regimes. Valley *et al.* [1994] have
 argued that original $\delta^{18}\text{O}$ zircon at time of forma-
 tion is preserved through amphibolite to granulite
 facies metamorphic conditions. Differences in zir-
 con core-rim $\delta^{18}\text{O}$ values of as much as 5.6‰ have
 been documented for Grenvillian zircons [Peck *et al.*,
 2003], and non-metamict “pristine” zircon has
 been shown to be resistant to hydrothermal alter-
 ation and oxygen isotope exchange at least at the
 biotite grade [e.g., King *et al.*, 1997]. Diffusion of
 oxygen in zircon has been explored experimentally
 under dry ($P_{\text{H}_2\text{O}} \sim 7$ MPa) and wet ($P_{\text{H}_2\text{O}} \geq 7$ MPa)
 conditions [Watson and Cherniak, 1997]. Results
 show that a zircon with a 100 μm effective diffu-
 sion radius can retain core $\delta^{18}\text{O}$ values at 900°C for
 65 Ma under dry conditions (applicable to granulite
 grade metamorphism), but under wet conditions,
 closure temperatures for oxygen isotopes are
 $\sim 650^\circ\text{C}$ for a cooling rate of 100°C/Ma and a
 diffusion radius of ~ 80 μm [Watson and Cherniak,
 1997]. In general, empirical observations and

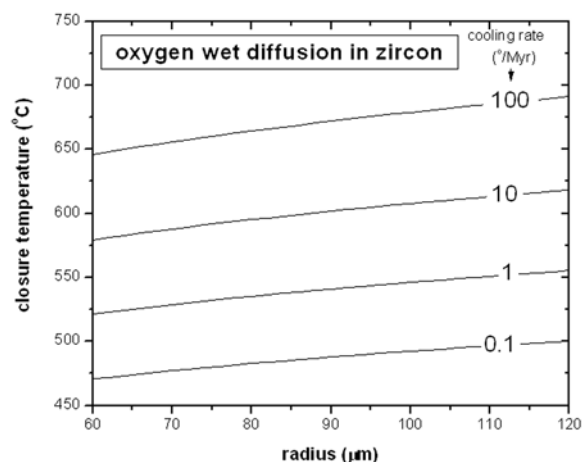


Figure 5. Bulk closure temperatures for oxygen diffusion in zircon, as a function of relevant zircon crystal radii (60–120 μm), under different cooling rates. Results were calculated using the Arrhenius relationship for wet oxygen diffusion in zircon [Watson and Cherniak, 1997].

822 experiment broadly agree that oxygen in zircon is
823 extremely retentive under dry conditions and that it
824 can be preserved under wet conditions, but prob-
825 ably not at temperatures much above $\sim 600^\circ\text{C}$.

826 [38] The circa 3.1 Ga postdepositional history of
827 sediments hosting Hadean zircons is not especially
828 well constrained; the only known widespread event
829 was a 2.7 Ga upper greenschist to lower amphib-
830 olite facies metamorphism [e.g., Pidgeon and
831 Wilde, 1998]. The JH metasediments are mature
832 (90–100% SiO_2), and quartz clasts have $\delta^{18}\text{O}$
833 values of +10–12‰ [Cavosie et al., 2005], as
834 much as 7‰ higher than Hadean JH zircons. Some
835 insight into oxygen isotope exchange can be
836 obtained from Figure 3.

837 [39] If the current degree of observed discordance
838 results from low temperature Pb^* loss (i.e., meta-
839 mictization), it is conceivable that grains which are
840 discordant today were either equally or more
841 susceptible to oxygen exchange in the 2.7 Ga
842 metamorphic event cited above. This logic is based
843 on the premise that grains which are metamict
844 and discordant today (most likely because of high
845 U and Th contents), would have been more likely
846 to be structurally damaged prior to the last known
847 widespread regional metamorphism. The fact that
848 these equally or more susceptible grains do not
849 trend toward host sediment values suggests that
850 substantial ^{18}O enrichment did not occur in more
851 pristine (>90% concordant) zircons presented in

Table 2. This analysis relies on evidence that is
somewhat tenuous, and without proper oxygen
diffusion profiles for these Hadean zircons, argu-
ments for and against diffusive oxygen exchange
cannot be evaluated further. However, zircons with
short diffusion radii ($<50 \mu\text{m}$; approximated by
analysis location in grain cross sections) contain
mantle $\delta^{18}\text{O}$ values (e.g., Figure 1, no. 11, 47, 48, 55).
This is not the expected result if the zircons
underwent substantial exchange with their host
sediments.

[40] Knowledge of the history of oxygen isotope
exchange in Hadean zircons is fundamentally ham-
pered by their unknown histories prior to deposi-
tion ($>3.1 \text{ Ga}$). Four Hadean zircons investigated
by high resolution ion microprobe depth profiles
(Trail et al., submitted manuscript, 2006) preserve
early Archean overgrowths and/or modifications of
Hadean cores. Ages less than or equal to 3.9 Ga
represent $\sim 10\text{--}15\%$ of the total grain radius
(typically 60–80 μm). The presence of overgrowths
or alteration zones on older preexisting zircon
cores opens the possibility that diffusive exchange
of oxygen may occurred. Closure temperatures for
oxygen in zircon as a function of crystal radii most
applicable to Jack Hills grain size distributions are
shown in Figure 5. Provided our interpretation of
the metamorphic history of the Jack Hills zircons is
correct (Trail et al., submitted manuscript, 2006),
we consider predepositional oxygen diffusion the
most plausible scenario for oxygen contamination
of Hadean zircons.

4.3. Ti-in-Zircon Thermometry

[41] Hadean zircons enriched in heavy oxygen were
used to argue for crust in chemical communication
with surface environments. The addition of water to
the zircon source melts will lower the eutectic
leading to low temperature melts. Calibration of
the $[\text{Ti}]_{\text{zircon}}$ thermometer [Watson and Harrison,
2005; Watson et al., 2006] places unique quantita-
tive constraints on zircon crystallization temper-
atures. Our new results reflect temperatures which
are consistent with minimum-melting granitoid-
type conditions reported by Watson and Harrison
[2005] and agree with other recent Hadean zircon
thermometry measurements [Watson and Harrison,
2006; Valley et al., 2006]. In addition, knowledge of
 $\delta^{18}\text{O}$ and crystallization temperature provides
enough information to make indirect calculations
of $\delta^{18}\text{O}$ values of other minerals present in the host
rocks. For example, empirical calculations per-
formed by Valley et al. [2003] show that crystalli-

905 zation of zircon with $\delta^{18}\text{O} = +6.0\text{--}6.5\text{‰}$, at the
 906 temperatures of $\sim 680\text{--}700^\circ\text{C}$ predicted by *Watson*
 907 *and Harrison* [2005], would co-exist with quartz
 908 at $\sim +9.0\text{‰}$. This value is also consistent with the
 909 O-isotopic composition of quartz in many granitic
 910 rocks [Taylor, 1968].

911 [42] The lowest $[\text{Ti}]_{\text{zircon}}$ measurement documented
 912 in this study was on a $\sim 40\%$ concordant grain,
 913 with a Ti concentration that corresponds to temper-
 914 atures as low as 588°C (Figure S1, no. 78) and
 915 consistent with a sub-solidus origin. However,
 916 since this grain shows evidence for substantial Pb
 917 loss, lower Ti concentrations could also reflect
 918 pervasive grain alteration. It is possible to estimate
 919 Ti diffusion for pristine zircon grains on the basis
 920 of the relatively systematic diffusion behavior
 921 observed for tetravalent cations in the zircon struc-
 922 ture as a function of ionic radius [Cherniak *et al.*,
 923 1997]. On the basis of this analysis, only temper-
 924 atures in excess of 1100°C are likely to lead to Ti
 925 diffusion in zircon over the diffusion length scales
 926 typical in Jack Hills zircons. This calculation
 927 agrees well with the recently derived Arrhenius
 928 equation from completed Ti diffusion experiments
 929 in zircon [Cherniak and Watson, 2006]. While
 930 there is no way to explicitly test for Ti diffusion,
 931 this zircon has a Th/U ratio of 3.2 that may be
 932 indicative of mobilization of U [Cavosie *et al.*,
 933 2004]. Since Ti diffuses at slightly lower temper-
 934 atures than U, it may have been mobilized and the
 935 low Ti-derived temperature record may be invalid.

937 4.4. Using Ti-in-Zircon Thermometry as a 938 Protolith Discriminator

939 [43] Alternative views have been presented which
 940 argue that the Ti thermometer cannot be used to
 941 constrain zircon provenance [Fu *et al.*, 2005;
 942 Kamber *et al.*, 2005; Nutman, 2006; Glikson,
 943 2006; Valley *et al.*, 2006; Coogan and Hinton,
 944 2006]. A criticism common to these reports is the
 945 concern over uncertainties in Zr and Ti activities in
 946 Hadean zircon source melts. For example, a late
 947 stage mafic melt may saturate the residual at low
 948 temperatures in Zr (and Si), to subsequently crys-
 949 tallize zircon. It was proposed that zircon crystal-
 950 lization temperatures could not be used to uniquely
 951 separate this process (or an analogous process)
 952 from granitic, water-saturated minimum melt con-
 953 ditions [Valley *et al.*, 2006; Coogan and Hinton,
 954 2006]. However, the current Ti data demonstrates
 955 that the majority of zircons crystallized from mafic
 956 sources (including late-stage residuals) are differ-
 957 ent in peak and distribution of the populations

[Watson *et al.*, 2006; Valley *et al.*, 2006], which 958
 argues against a common origin [Harrison *et al.*, 959
 2006, 2007; Watson and Harrison, 2006]. It was 960
 also suggested that tonalites could crystallize zir- 961
 cons at temperatures indistinguishable from mini- 962
 mum melt conditions implied for the Hadean source 963
 rocks [Nutman, 2006]. This possibility for the 964
 majority of Hadean zircon is ruled out because 965
 saturation temperatures in tonalitic melts are 966
 demonstrably higher than the $680 \pm 25^\circ\text{C}$ peak 967
 observed for Hadean zircons [Harrison *et al.*, 968
 2006]. Finally, it was recently shown by calculation 969
 and geologic example that igneous rocks formed at 970
 higher temperatures ($>750^\circ\text{C}$) produce Ti-derived 971
 temperatures well above the wet granite solidus 972
 [Harrison *et al.*, 2007]. However, a minor compo- 973
 nent ($<10\%$) of the Hadean zircons thus far ana- 974
 lyzed could have been derived from a TTG-type 975
 melt on the basis of $\sim 750^\circ\text{C}$ crystallization temper- 976
 atures in some grains. 977

[44] The Ti thermometer applies directly to sys- 978
 tems which contain a pure TiO_2 phase (e.g., rutile), 979
 but suitably to melts with a Ti-saturated phase (e.g., 980
 ilmenite). Since Ti-activity is not strictly quantified 981
 in JH source melts, it was argued that measured 982
 temperatures could reflect Ti melt activity <1 rather 983
 than granitic minimum melt conditions [Nutman, 984
 2006; Coogan and Hinton, 2006]. However, melts 985
 that contain high activities of Zr required for zircon 986
 saturation generally contain high activities of Ti. 987
 Ti-activity in melts has been characterized for 988
 magmas of diverse compositions [Ryerson and 989
 Watson, 1987], and more recently among siliceous 990
 melts such as trondjemite, s-type granite, and 991
 metaluminous granite [Hayden *et al.*, 2005]. 992
 Results have shown that a siliceous melt, indepen- 993
 dent of water content, will often saturate in a Ti 994
 bearing phase before zircon [Ryerson and Watson, 995
 1987; Hayden *et al.*, 2005]. This reasoning relies 996
 on the expectation that Hadean zircon source melts 997
 have high SiO_2 activity. This is substantiated 998
 because many SiO_2 inclusions have been discov- 999
 ered in all Hadean zircon inclusion studies to date 1000
 [Maas *et al.*, 1992; Peck *et al.*, 2001; Trail *et al.*, 1001
 2004; Cavosie *et al.*, 2004; Crowley *et al.*, 2005]. It 1002
 is worth noting though that melts with low Si-activity 1003
 would only serve to compensate for sub-unity 1004
 Ti activity [Ferry and Watson, 2007]. 1005

[45] Data have been shifted to show the effect of 1006
 sub-unity Ti activity in the initial publication 1007
 presenting the thermometer [Watson and Harrison, 1008
 2005] and more recently by Coogan and Hinton 1009
 [2006] during their comparison of 15 zircons from 1010

1011 five oceanic gabbros. As demonstrated by *Coogan*
 1012 *and Hinton* [2006] direct comparison of the two
 1013 populations shows they are dissimilar. *Coogan and*
 1014 *Hinton* [2006] drew an arrow in their Figure 1 to
 1015 show the shift in crystallization temperatures for
 1016 Hadean zircons if the source melts had Ti activity of
 1017 0.5, perhaps to imply that an overlap exists with
 1018 their temperature data. We disagree with this com-
 1019 parison simply because all five gabbros in their
 1020 study crystallized in the presence of ilmenite, which
 1021 implies sub-unity Ti-activity, so that a sub-unity
 1022 shift must be applied the data of *Coogan and*
 1023 *Hinton* [2006] as well. Studies that have explored
 1024 zircon crystallization in the presence of ilmenite
 1025 have previously yielded Ti-activities of ~ 0.6
 1026 [Watson *et al.*, 2006]. The uncertainties of the Ti
 1027 thermometer when applied to zircons of unknown
 1028 origin can be reasonably constrained, and it remains
 1029 clear that results that bear on conditions of Hadean
 1030 zircon crystallization are reproducible [Watson and
 1031 Harrison, 2006].

1033 4.5. Hadean Zircon Rare Earth Element 1034 Partitioning

1035 [46] It has generally been assumed that Hadean
 1036 zircons are magmatic, a basis for the interpretation
 1037 of our data. Here, we apply the lattice strain
 1038 theory of partitioning to rare earth elements
 1039 (REEs) in zircon, a model which is intended for
 1040 application to crystal-melt partitioning [Blundy
 1041 and Wood, 1994]. In other words, REEs of meta-
 1042 morphic (or hydrothermal) zircon are expected to
 1043 show deviations from the parabolic behavior of
 1044 partition coefficients versus ion radii of substituent
 1045 ions, if partition coefficients are calculated from
 1046 magmatic compositions. In this section, we show
 1047 that the lattice strain model can help distinguish
 1048 magmatic from metamorphic/hydrothermal zir-
 1049 cons, and conclude that Hadean zircons are dom-
 1050 inantly magmatic (sections 4.5.1 and 4.5.2). We
 1051 further discuss whether REE patterns of Hadean
 1052 zircons can be employed for provenance determi-
 1053 nations (section 4.5.3).

1054 [47] To achieve this, we have compiled 73 published
 1055 REE concentrations from 51 Hadean zircons [Maas
 1056 *et al.*, 1992; Wilde *et al.*, 2001; Peck *et al.*, 2001;
 1057 Crowley *et al.*, 2005]. In an attempt to match zircon
 1058 provenance, various generic whole rock REE com-
 1059 positions of magmatic origin were used to approx-
 1060 imate REE melt concentrations, and to calculate
 1061 hypothetical REE zircon partition coefficients. The
 1062 model compositions chosen for this analysis, from
 1063 felsic to more mafic were: Archean granite [Condie,

1064 1993], Archean tonalite-trondhjemite-granodiorite
 [Condie, 1993], adakite [Samsonov *et al.*, 2005],
 1065 anorthosite [Markl, 2001] and N-type MORB [Sun
 1066 and McDonough, 1989]. The lattice strain equation
 1067 was then fit to the five sets of partition coefficients
 1068 for each of the 73 REE measurements, assuming
 1069 average $T = 680^\circ\text{C}$ for Hadean zircons. In this
 1070 calculation, $r_o = 0.84$?, D_o and E are free parameters
 1071 and were allowed to vary during curve fitting. The
 1072 best-fit among the candidate rock types was deter-
 1073 mined simply by comparing the R^2 values. It is
 1074 worth noting that changing the crystallization tem-
 1075 perature will not change the R^2 value of a fit, but will
 1076 change E . 1077

[48] We have evaluated this approach by selecting
 1078 zircons from a variety of host rocks of known
 1079 provenance, including rock types which were not
 1080 included in our five model compositions [Hoskin,
 1081 1998, 2005; Hoskin and Black, 2000; Hoskin and
 1082 Ireland, 2000; Dawson *et al.*, 2001; Rubatto, 2002;
 1083 Whitehouse and Platt, 2003; Whitehouse and
 1084 Kamber, 2003, 2005; Pettke *et al.*, 2005]. In
 1085 this way, 68 magmatic, 47 metamorphic, and 24
 1086 “hydrothermal” published zircon REE data were
 1087 fit to the lattice strain model using our five host
 1088 rock types (Table S4). 1089

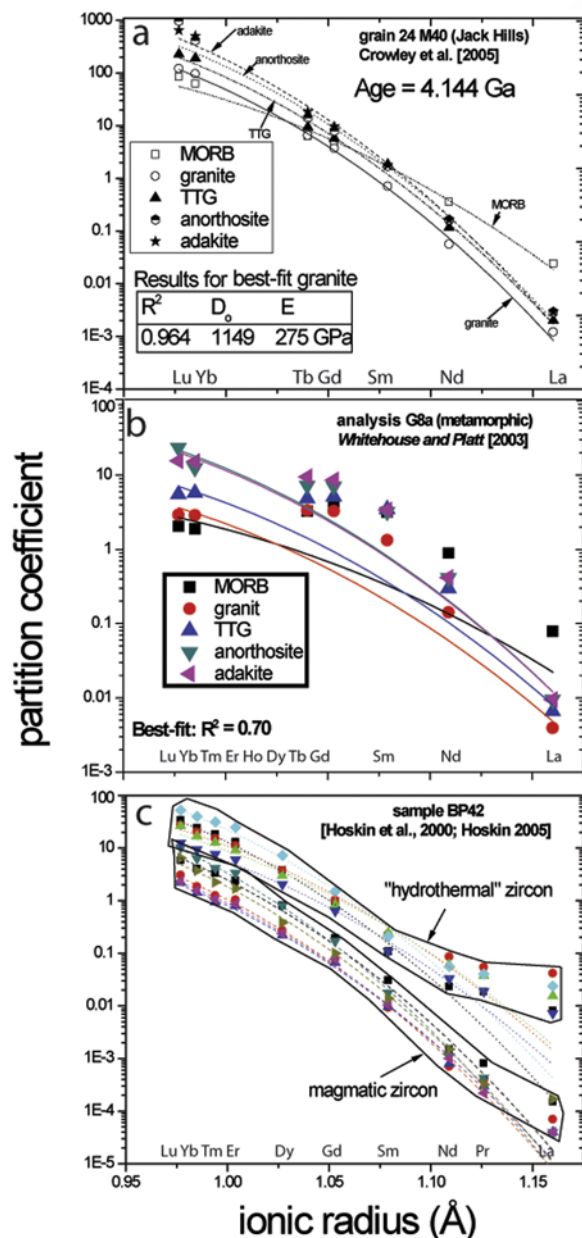
1090 4.5.1. Magmatic Versus Metamorphic 1091 Zircon

[49] The usefulness of CL images as a guide for
 1092 selecting analysis spots for ion microprobe was
 1093 demonstrated by correlation between high $\delta^{18}\text{O}$
 1094 zircons with zones typically interpreted as mag-
 1095 matic [Cavosie *et al.*, 2005]. Although cathodolu-
 1096 minescence images are informative, interpretations
 1097 can be subjective and the suite of textures inferred
 1098 to be magmatic versus metamorphic can be am-
 1099 biguous [Corfu *et al.*, 2003]. Because of this
 1100 ambiguity, Cavosie *et al.* [2005] and Nemchin *et*
 1101 *al.* [2006a] chose to err on the side of caution and
 1102 reject from consideration Hadean zircons which do
 1103 not characteristic magmatic zoning as deduced
 1104 from CL images. 1105

[50] Derived REE partition coefficients for igneous
 1106 versus metamorphic zircon show a definite quanti-
 1107 fiable difference between the two. Our application
 1108 of the lattice-strain model shows that the average
 1109 best-fit R^2 value for 68 igneous zircons is $0.89 \pm$
 1110 0.07 (1σ). This is in contrast to our analysis of
 1111 47 metamorphic zircons (or metamorphic grain
 1112 regions) which have an average best-fit R^2 value
 1113 of 0.67 ± 0.15 . The results provide a baseline for
 1114 comparison to Hadean zircons, which have an
 1115

1116 average best-fit R^2 value of 0.88 ± 0.06 , highly
1117 suggestive of an igneous origin. As a visual exam-
1118 ple, Figure 6a shows the lattice strain function
1119 curves fit to the five partition coefficient sets for a
1120 Jack Hills zircon, to show the parabolic behavior
1121 common among the 68 igneous test cases. For
1122 comparison, representative partition coefficient sets
1123 from the five attempted host rocks fits are shown for
1124 a metamorphic zircon from the granulite-grade
1125 garnet gneiss near the Carratraca peridotite massif
1126 (Figure 6b). Partition coefficients versus ion radii
1127 for the metamorphic grain region shows deviations
1128 from predicted magmatic partitioning (compare to
1129 Figure 6a). This example, along with others, sug-

gests that (hypothetical) partition coefficients of
metamorphic zircons calculated from igneous host
rocks are unlikely to mimic the parabolic behavior
seen for magmatic zircon-melt partitioning [e.g.,
Manning et al., 2006]. We find in our analysis that
Hadean zircons (with very few exceptions; see
section 4.5.2) are reconcilable with a magmatic
origin. A noteworthy feature of some metamorphic
zircons is that they show flat partitioning of HREEs,
a common feature of zircons which crystallized in
the presence of garnet [e.g., *Whitehouse and Platt,*
2003; Rubatto, 2002]. This type of partitioning is
not present in Hadean zircons which would seem to
indicate that the grains did not form in the presence
of garnet.



4.5.2. Hydrothermal Modification of Hadean Zircon

[51] *Hoskin [2005]* proposed that metamict zones
of Hadean zircons could have been enriched in
heavy oxygen and LREE during postprimary
crystallization by hydrothermal fluids. Despite
crystallization ages that were indistinguishable in
different domains of complex zircons, that study
found high concentrations of LREE in “hydrother-
mal” mantles relative to igneous cores in zircons
from the Boggy Plain zoned pluton in eastern
Australia. The preferred model for these features
was that later fluids imparted high $^{18}\text{O}/^{16}\text{O}$ ratios to
the zircons and were responsible for the enriched

Figure 6. (a) Partition coefficient sets versus ionic radius (\AA) for different host rock candidates of a representative Hadean zircon. We used the *Blundy and Wood [1994]* lattice strain model and a crystallization temperature of 680°C [*Watson and Harrison, 2006*], and best host rock fit was resolved by the R^2 value. In this particular grain from *Crowley et al. [2005]*, the best fit was Archean granite [*Condie, 1993*]. (b) Representative REE partition coefficients for our five host rocks calculated for a metamorphic grain region [*Whitehouse and Platt, 2003*]. This metamorphic grain region, like others (Table S4), shows that partition coefficients derived from igneous rocks deviate from the lattice strain model. The color-correlated lines correspond to attempted fits to the partition coefficients. (c) Trace element partition coefficients of magmatic and hydrothermal zircon from aplite sample BP42 [*Hoskin, 2005*]. Hydrothermal zircons show REE deviation in partition coefficients relative to magmatic zircons, most noticeable in La, Pr, and Nd. In this particular case, our five host rocks were not used because whole rock concentrations were available from *Hoskin et al. [2000]*. The lattice strain model has an average magmatic fit of $R^2 = 0.89$ ($n = 5$) and a hydrothermal fit of $R^2 = 0.76$ ($n = 5$).

1159 LREE patterns as well. In this scenario, plate
 1160 boundary processes would be unnecessary to ac-
 1161 count for high $\delta^{18}\text{O}$ zircon values in the Hadean
 1162 [Hoskin, 2005]. Experimental work supports this
 1163 proposal since hydrothermal annealing of metamict
 1164 zircon is possible at 350°C or lower [e.g., Geisler
 1165 *et al.*, 2003].

1166 [52] At the time when the Hoskin [2005] manu-
 1167 script was submitted (Dec. 2003), only one CL
 1168 image of a Jack Hills zircon with ion microprobe
 1169 oxygen spots [Wilde *et al.*, 2001; Peck *et al.*, 2001]
 1170 and two other Hadean zircon images [Nelson *et al.*,
 1171 2000] were published. Therefore conclusions that
 1172 supported a hydrothermal origin for altered Hadean
 1173 zircons arose on the basis of a few CL images as
 1174 well as high $\delta^{18}\text{O}$ values (+10‰) for one (discor-
 1175 dant) zircon core [Mojzsis *et al.*, 2001]. There now
 1176 exists a large data set of published Hadean zircon
 1177 CL images [Cavosie *et al.*, 2004, 2005; Dunn *et al.*,
 1178 2005; Crowley *et al.*, 2005] (Figures 1 and S1),
 1179 many of which display concentric zoning usually
 1180 ascribed to a magmatic origin [Cavosie *et al.*,
 1181 2004]. Some zircons with concentric zones record
 1182 $\delta^{18}\text{O}$ zircon well above mantle values, which do not
 1183 appear to lend support to the annealing hypothesis
 1184 as an important process for ^{18}O enrichment in these
 1185 grains. Other studies have shown that hydrothermal
 1186 zircons (or hydrothermally altered regions) are
 1187 frequently enriched in Hf, usually by $\geq 2\%$ [e.g.,
 1188 Kerrich and King, 1993; Hoskin, 2005]. Out of
 1189 135 analyses which specifically characterized
 1190 Hadean zircons for Hf [Maas *et al.*, 1992; Cavosie
 1191 *et al.*, 2005; Crowley *et al.*, 2005] average concen-
 1192 trations are 0.94% (range = 0.66–1.4%).

1193 [53] We sought to evaluate whether the lattice strain
 1194 model can be used to distinguish between igneous
 1195 zircon and zircon grain regions annealed by hydro-
 1196 thermal fluids. Rare earth element partition coeffi-
 1197 cients were fit to the lattice strain function in the
 1198 same manner discussed above for 24 hydrothermal
 1199 zircons [Hoskin, 2005; Pettke *et al.*, 2005]. Results
 1200 show hydrothermal zircons have a best-fit R^2 aver-
 1201 age of 0.78 ± 0.05 . For comparison, Figure 6c shows
 1202 hydrothermal and igneous zircons from sample
 1203 BP42 [Hoskin, 2005; Hoskin *et al.*, 2000]. It is
 1204 evident that hydrothermal zircon shows large parti-
 1205 tion coefficient deviations compared to magmatic
 1206 zircon, a phenomenon seen in only 3 of 73 Hadean
 1207 zircon REE analyses explored here (i.e., $R^2 < 0.78$;
 1208 see Tables S4 and S5). With few exceptions, calcu-
 1209 lated REE partition coefficients in Hadean zircons
 1210 do not to deviate from the lattice strain model.
 1211 Unless the assumptions of the lattice strain model

have been violated, we can conclude that the 1212
 majority of Hadean zircons with LREE-enriched 1213
 concentrations, likely preserve a signature from 1214
 their primary magmatic values. 1215

[54] To summarize, in concert with the Ti data 1216
 [Watson and Harrison, 2005] and image analysis 1217
 [e.g., Cavosie *et al.*, 2004], we have found that the 1218
 vast majority ($\sim 95\%$) of Hadean zircons are mag- 1219
 matic. However, we are not confident that we can 1220
 unambiguously distinguish between metamorphic 1221
 versus hydrothermal zircon solely on the basis of 1222
 the above analysis. 1223

4.5.3. Provenance Discrimination 1224

[55] Maas *et al.* [1992] demonstrated that REE 1225
 concentrations in Hadean zircons show marked 1226
 enrichment in LREE, similar to zircon compositions 1227
 from Phanerozoic diorites and granites. Follow-up 1228
 $\delta^{18}\text{O}$ zircon measurements along with REE studies 1229
 of JH zircons by Wilde *et al.* [2001] and Peck *et al.* 1230
 [2001] showed that correlative high $\delta^{18}\text{O}$ zircon 1231
 values with enriched LREEs appear consistent with 1232
 zircons derived from granitoid-type source rocks. In 1233
 another study, trace element patterns and U concen- 1234
 trations of Hadean and early Archean detrital zir- 1235
 cons from Mount Narryer were used to argue that the 1236
 MN grains were derived from evolved granitic 1237
 rocks, but that the JH zircons are not [Crowley *et* 1238
al., 2005]. 1239

[56] Whitehouse and Kamber [2002] challenged 1240
 these interpretations on the basis of their analysis 1241
 of circa 3.81 Ga zircons from a West Greenland 1242
 orthogneiss sample. In their study, it was assumed 1243
 that the rock was pristine and that whole rock 1244
 REE values reliably reflect magmatic REE abun- 1245
 dances at time of emplacement. Because LREE 1246
 abundances measured in the whole rock and the 1247
 zircons appeared to be inconsistent with predicted 1248
 partition coefficients for zircon-melt, Whitehouse 1249
 and Kamber [2002] concluded that models which 1250
 derive source melt characteristics from zircon 1251
 alone are not reliable. 1252

[57] To explore this further, Figure 6a illustrates the 1253
 variability in partition coefficients depending on 1254
 different model melt compositions for a selected 1255
 Hadean zircon. In this specific case, best-fit results 1256
 for the lattice-strain parabola according to Blundy 1257
 and Wood [1994] favor a granitic protolith. Of the 1258
 70 published Hadean zircon REE patterns inter- 1259
 preted as magmatic (i.e., excluding the 3 with 1260
 $R^2 < 0.78$), we found 26 best-fits for granite, 24 1261
 for tonalite-trondhjemite-granodiorites, 7 for adakite, 1262

1263 1 for anorthosite, and 12 for N-type MORB
1264 (Table S4). This calculation seems appealing at
1265 first because a significant population of zircons
1266 indicate REE partitioning consistent with crystalli-
1267 zation from a granitoid-type melt. However, during
1268 our investigation, we found the lattice-strain theory
1269 sometimes predicts protolith REE compositions for
1270 zircons of known provenance that are better fits
1271 with rocks for a different lithology.

1272 [58] For example, 6 zircons from two separate
1273 felsic metagranitoids [Hoskin and Black, 2000]
1274 predicted granite (4×), TTG (1×), adakite (1×)
1275 as the host rocks. In another case, zircons analyzed
1276 from a quartz diorite [Whitehouse and Kamber,
1277 2003] produced granite (6×), TTG (5×), MORB
1278 (1×), and adakite (1×) as the host rock solutions.
1279 The MADRID zircon taken from an ultramafic
1280 rock ascribed a kimberlitic origin [Hoskin, 1998;
1281 Dawson et al., 2001] predicted host rocks of
1282 adakite (3×), anorthosite (3×), and TTG (1×).
1283 The last result broadly supports our model because
1284 no kimberlitic rock was included in our host rock
1285 matches, yet appropriately, the model still generally
1286 predicted a mafic rather than felsic end-member. An
1287 analogous result was achieved for a harzburgite
1288 xenolith [Dawson et al., 2001] which returned best
1289 fits for an anorthosite host rock for all 17 zircons.

1290 [59] Since the partition model sometimes predicts
1291 rocks that the zircons did not form in, we cannot be
1292 confident about specific assignment of a protolith
1293 based exclusively on this model. However, if we
1294 generalize our five rock-types into felsic (granite
1295 and TTG) versus mafic (adakite, anorthosite,
1296 MORB) for zircons of known provenance, then
1297 the zircon parentage is correctly classified ~80%
1298 of the time. Given these results, we can propose
1299 that REE partitioning indicates a felsic ($n = 50$)
1300 rather than a mafic ($n = 20$) end-member for the
1301 majority of Hadean zircons thus far studied. The
1302 results of section 4.5.3 should be considered a
1303 qualitative guide that lends support to other more
1304 quantitative lines (O-isotopes, Ti, mineral inclu-
1305 sions) for a dominantly granitic rather than mafic
1306 origin of most Hadean zircons.

1308 5. Summary

1309 [60] Of the $\delta^{18}\text{O}$ zircon measurements reported
1310 here on 89 pre-3.8 Ga zircons, 50 of these grains
1311 were free of analytical artifacts resulting from
1312 cracks, correlatable by CL with geochronology
1313 spots, and $\geq 90\%$ concordant. Of these 50 grains,
1314 15 analyses contained $\delta^{18}\text{O}$ values out of equilib-

rium with a pure mantle source end-member 1315
($\geq 6.0\%$), five of which were above $+6.5\%$. In 1316
agreement with previous results [e.g., *Mojzsis et* 1317
al., 2001; *Peck et al.*, 2001; *Cavosie et al.*, 2005] 1318
we find that approximately 25% of pre-3.8 Ga 1319
grains so far analyzed preserve resolvable ^{18}O 1320
enrichments above mantle equilibrium values. We 1321
analyzed a number of variably concordant zircons 1322
to search for trends in $\delta^{18}\text{O}$ zircon and U/Pb% 1323
concordance and found that counter to expectation, 1324
more discordant zircons do not tend toward aver- 1325
age sediment values of $+10$ – 12% . 1326

[61] Independently, our Ti measurements on select- 1327
ed zircons reflect crystallization temperatures con- 1328
sistent with the hypothesis that most Hadean 1329
zircons were sourced from low temperature, min- 1330
imum melt conditions. Such conditions are best 1331
satisfied by water-saturated granitoid-type sources 1332
[*Watson and Harrison*, 2005, 2006; *Harrison et* 1333
al., 2007]. The one exception provided temper- 1334
atures which ranged from 588 – 629°C . This is the 1335
lowest temperature recorded for Hadean zircon 1336
thus far, and while the discordant nature of the 1337
grain calls into question the validity of using Ti 1338
concentration to reflect on the true crystallization 1339
temperature, the result is consistent with our REE 1340
analysis which indicated very small component of 1341
Hadean zircon source rocks are not of igneous 1342
origin. 1343

[62] In addition, we have evaluated scenarios 1344
which have been presented as alternatives to the 1345
granite theory of Hadean zircon petrogenesis [e.g., 1346
Whitehouse and Kamber, 2002; *Hoskin*, 2005]. 1347
These studies based their conclusions on analysis 1348
of REE in zircon from specific case examples, and 1349
to follow-up on that work we have compiled REE 1350
data from Hadean zircons in an attempt to match 1351
these to various host lithotypes using the *Blundy* 1352
and Wood [1994] lattice-strain model. We find that 1353
(1) there is broad support for view that Hadean 1354
zircons are dominantly of felsic provenance; (2) the 1355
partitioning of REE constrains Hadean zircons 1356
as being almost entirely ($>95\%$) magmatic; and 1357
(3) hydrothermal modification of Hadean zircon 1358
(leading to high $\delta^{18}\text{O}$ zircon and enriched LREE) is 1359
rare or absent in the samples thus far described. 1360

[63] We conclude, on the basis of the several lines 1361
of evidence discussed above, that unless that 1362
Hadean Earth operated in a manner fundamentally 1363
different from all that we know, the simplest 1364
explanation for all observed data is that an evolved 1365
rock cycle that included the pervasive activity of 1366

1367 liquid water in the context of formation of granitic
1368 crust was present on Earth by 4.3–4.2 Ga.

1369 Acknowledgments

1370 [64] Support from the NASA Exobiology Program (NAG5-
1371 13497) “Mission to Really Early Earth” to S.J.M., the NASA
1372 Astrobiology Institute, the NSF Instrumentation and Facilities
1373 Program, and Australian Research Council to T.M.H. are
1374 greatly appreciated. D.T. gratefully acknowledges fellowship
1375 support from the Alfred P. Sloan Foundation. The ion micro-
1376 probe facility at UCLA is partly supported by a grant from the
1377 Instrumentation and Facilities Program, Division of Earth
1378 Sciences, National Science Foundation. O. M. Lovera (UCLA)
1379 provided assistance with Kolmogorov-Smirnov calculations.
1380 G. B. Morgan and D. London (OU) are thanked for assistance
1381 with CL imaging. N. L. Cates assisted with data collection.
1382 The unpublished Ti diffusion data for zircon made available by
1383 D. J. Cherniak are much appreciated. This manuscript benefit-
1384 ed from discussion with E. J. Catlos, A. J. Cavosie, and
1385 P. Holden, the constructive and very thorough comments of
1386 three anonymous reviewers, and helpful suggestions from the
1387 handling editor, V. J. M. Salters.

1389 References

1390 Amelin, Y. (2005), A tale of early Earth told in zircons,
1391 *Science*, *310*, 1914–1915.
1392 Benninghoven, A., F. G. Rüdener, and H. W. Werner (1987),
1393 *Secondary Ion Mass Spectrometry: Basic Concepts, Instru-*
1394 *mental Aspects, Applications and Trends*, 1227 pp., John
1395 Wiley, Hoboken, N. J.
1396 Bibikova, Y. V., V. I. Ustinov, T. V. Gracheva, M. A. Kiselevskiy,
1397 and Y. A. Shukolyukov (1982), Variations of isotopic composi-
1398 tion of oxygen in accessory zircons, *Dokl. Akad. Nauk SSSR*,
1399 *264*, 698–700.
1400 Bindeman, I. N., and J. W. Valley (2001), Low- $\delta^{18}\text{O}$ rhyolites
1401 from Yellowstone: Magmatic evolution based on analyses of
1402 zircons and individual phenocrysts, *J. Petrol.*, *42*, 1491–
1403 1517.
1404 Black, L. P., et al. (2004), Improved $^{206}\text{Pb}/^{238}\text{U}$ microprobe
1405 geochronology by the monitoring of a trace-element-related
1406 matrix effect; SHRIMP, ID-TIMS, ELA-ICP-MS and oxygen
1407 isotope documentation for a series of zircon standards,
1408 *Chem. Geol.*, *205*, 115–140.
1409 Bleeker, W. (2004), Towards a “natural” time scale for the
1410 Precambrian: A proposal, *Lethaia*, *37*, 219–222.
1411 Blundy, J., and B. Wood (1994), Prediction of crystal-melt
1412 partition coefficients for elastic moduli, *Nature*, *372*, 452–454.
1413 Booth, A. L., Y. Kolodny, C. P. Chamberlain, M. McWilliams,
1414 A. K. Schmitt, and J. Wooden (2005), Oxygen isotopic com-
1415 position and U-Pb discordance in zircon, *Geochim. Cosmo-*
1416 *chim. Acta*, *69*, 4895–4905.
1417 Bowring, S. A., and I. S. Williams (1999), Priscoan (4.00–
1418 4.03 Ga) orthogneisses from northwestern Canada, *Contrib.*
1419 *Mineral. Petrol.*, *134*, 3–16.
1420 Caro, G., V. C. Bennett, B. Bourdon, T. M. Harrison, and S. J.
1421 Mojzsis (2006), The ^{142}Nd record of Hadean zircons
1422 (abstract), *Geochim. Cosmochim. Acta.*, *70*, A85.
1423 Cates, N. L., and S. J. Mojzsis (2006), Chemical and isotopic
1424 evidence for widespread Eoarchean (≥ 3750 Ma) metasedi-
1425 mentary enclaves in southern West Greenland, *Geochim.*
1426 *Cosmochim. Acta*, *70*, 4229–4257.

Cavosie, A. J., S. A. Wilde, D. Y. Liu, P. W. Weiblen, and J. W. 1427
Valley (2004), Internal zoning and U-Th-Pb chemistry of 1428
Jack Hills detrital zircons: A mineral record of early Archean 1429
to Mesoproterozoic (4348–1576 Ma) magmatism, *Precambrian Res.*, *135*, 251–279. 1430
1431
Cavosie, A. J., J. W. Valley, S. A. Wilde, and Edinburg Ion 1432
Microphone Facility (2005), Magmatic $\delta^{18}\text{O}$ in 4400– 1433
3900 Ma detrital zircons: A record of the alteration and 1434
recycling of crust in the early Archean, *Earth Planet. Sci.* 1435
Lett., *235*, 663–681. 1436
Cherniak, D. J., and E. B. Watson (2000), Pb diffusion in 1437
zircon, *Chem. Geol.*, *172*, 5–24. 1438
Cherniak, D. J., and E. B. Watson (2006), Ti diffusion in 1439
zircon, *Eos Trans. AGU*, *87*(52), Fall Meet. Suppl., Abstract 1440
V31F-02. 1441
Cherniak, D. J., J. M. Hanchar, and E. B. Watson (1997), 1442
Diffusion of tetravalent cations in zircon, *Contrib. Mineral.* 1443
Petrol., *127*, 383–390. 1444
Compston, W., and R. T. Pidgeon (1986), Jack Hills, evidence 1445
of more very old detrital zircons in Western Australia, *Nature*, 1446
321, 766–769. 1447
Condie, K. C. (1993), Chemical composition and evolution of 1448
the upper continental crust: Contrasting results from surface 1449
samples and shales, *Chem. Geol.*, *104*, 1–37. 1450
Coogan, L. A., and R. W. Hinton (2006), Do trace element 1451
compositions of detrital zircons require Hadean continental 1452
crust?, *Geology*, *34*, 633–636. 1453
Corfu, F., J. M. Hanchar, P. W. O. Hoskin, and P. Kinny (2003), 1454
Atlas of zircon textures, *Rev. Mineral. Geochem.*, *53*, 468–500. 1455
Crowley, J. L., J. S. Myers, P. J. Sylvester, and R. A. Cox 1456
(2005), Detrital zircon from the Jack Hills and Mount 1457
Narryer, Western Australia: Evidence for diverse >4.0 Ga 1458
source rocks, *J. Geol.*, *113*, 239–263. 1459
Dawson, J. B., P. G. Hill, and P. D. Kinny (2001), Mineral 1460
chemistry of a zircon-bearing, composite, veined and meta- 1461
somatised upper-mantle peridotite xenolith from kimberlite, 1462
Contrib. Mineral. Petrol., *140*, 720–733. 1463
Dunn, S. J., A. A. Nemchin, P. A. Cawood, and R. T. Pidgeon 1464
(2005), Provenance record of the Jack Hills metasedimentary 1465
belt: Source of the Earth’s oldest zircons, *Precambrian Res.*, 1466
138, 235–254. 1467
Ferry, J. M., and E. B. Watson (2007), New thermodynamic 1468
models and revised calibrations for the Ti-in-zircon and 1469
Zr-in-rutile thermometers, *Contrib. Mineral. Petrol.*, in press. 1470
Froude, D. O., T. R. Ireland, P. D. Kinny, I. S. Williams, 1471
W. Compston, and J. S. Myers (1983), Ion microprobe iden- 1472
tification of 4,100–4,200 Myr-old terrestrial zircons, *Nature*, 1473
304, 616–618. 1474
Fu, B., A. J. Cavosie, C. C. Clechenko, J. Fournelle, N. T. 1475
Kita, J. Lackey, F. Page, S. A. Wilde, and J. W. Valley 1476
(2005), Ti-in-zircon thermometer: Preliminary results, *Eos* 1477
Trans. AGU, *86*(52), Fall Meet. Suppl., Abstract V41F-1538. 1478
Geisler, T., R. T. Pidgeon, R. Kurtz, W. van Bronswijk, and 1479
H. Schleicher (2003), Experimental hydrothermal alteration 1480
of partially metamict zircon, *Am. Mineral.*, *88*, 1496–1513. 1481
Glikson, A. (2006), Comment on “Zircon thermometer reveals 1482
minimum melting conditions on earliest Earth” I, *Science*, 1483
311, 779a, doi:10.1126/science.1120073. 1484
Harrison, T. M., J. Blichert-Toft, W. Müller, F. Albarede, 1485
P. Holden, and S. J. Mojzsis (2005a), Heterogeneous Hadean 1486
hafnium: Evidence of continental crust at 4.4 to 4.5 Ga, 1487
Science, *310*, 1947–1950. 1488
Harrison, T. M., A. Aikman, P. Holden, A. M. Walker, 1489
C. McFarlane, D. Rubatto, and E. B. Watson (2005b), Test- 1490
ing the Ti-in-zircon thermometer, *Eos Trans. AGU*, *86*(52), 1491
Fall Meet. Suppl., Abstract V41F-1540. 1492

- 1493 Harrison, T. M., J. Blichert-Toft, W. Müller, F. Albaredo,
1494 P. Holden, and S. J. Mojzsis (2006), Response to comment
1495 on “Heterogeneous Hadean hafnium: Evidence of continen-
1496 tal crust at 4.4 to 4.5 Ga”, *Science*, *312*, 1139b, doi:10.1126/
1497 science.1125408.
- 1498 Harrison, T. M., E. B. Watson, and A. K. Aikman (2007),
1499 Temperature spectra of zircon crystallization in plutonic
1500 rocks, *Geology*, in press.
- 1501 Hayden, L. A., E. B. Watson, and D. A. Wark (2005), Rutile
1502 saturation and TiO₂ diffusion in hydrous siliceous melts, *Eos*
1503 *Trans. AGU*, *86*(52), Fall Meet. Suppl., Abstract MR13A-
1504 0076.
- 1505 Hoskin, P. W. O. (1998), Minor and trace element analysis of
1506 natural zircon (ZrSiO₄) by SIMS and laser ablation ICPMS:
1507 A consideration and comparison of two broadly competitive
1508 techniques, *J. Trace Microprobe Tech.*, *16*, 301–326.
- 1509 Hoskin, P. W. O. (2005), Trace-element composition of hydro-
1510 thermal zircon and the alteration of Hadean zircon from the Jack
1511 Hills, Australia, *Geochim. Cosmochim. Acta*, *69*, 637–648.
- 1512 Hoskin, P. W. O., and L. P. Black (2000), Metamorphic zircon
1513 formation by solid-state recrystallization of protolith igneous
1514 zircon, *J. Metamorph. Geol.*, *18*, 423–439.
- 1515 Hoskin, P. W. O., and T. R. Ireland (2000), Rare earth element
1516 chemistry of zircon and its use as a provenance indicator,
1517 *Geology*, *28*, 627–630.
- 1518 Hoskin, P. W. O., P. D. Kinny, D. Wyborn, and B. W. Chappell
1519 (2000), Identifying accessory mineral saturation during dif-
1520 ferentiation in granitoid magmas: An integrated approach,
1521 *J. Petrol.*, *41*, 1365–1396.
- 1522 Iizuka, T., K. Horie, T. Komiya, S. Maruyama, T. Hirata,
1523 H. Hidaka, and B. F. Windley (2006), 4.2 Ga zircon xeno-
1524 cryst in an Acasta gneiss from northwestern Canada: Evid-
1525 ence for early continental crust, *Geology*, *34*, 245–248.
- 1526 Kamber, B. S., M. J. Whitehouse, R. Bolhar, and S. Moorbath
1527 (2005), Volcanic resurfacing and the early terrestrial crust:
1528 Zircon U-Pb and REE constraints from the Isua Greenstone
1529 Belt, southern West Greenland, *Earth Planet. Sci. Lett.*, *240*,
1530 276–290.
- 1531 Kemp, A. I. S., C. J. Hawkesworth, B. A. Paterson, and P. D.
1532 Kinny (2006), Episodic growth of the Gondwana supercon-
1533 tinent from hafnium and oxygen isotopes in zircon, *Nature*,
1534 *439*, 580–583.
- 1535 Kerrich, R., and R. King (1993), Hydrothermal zircon and
1536 baddeleyite in Val d’Or Archean mesothermal gold deposits
1537 characteristics, compositions and fluid-inclusion properties,
1538 with implications for timing of primary gold mineralization,
1539 *Can. J. Earth Sci.*, *30*, 2334–2352.
- 1540 King, E. M., C. T. Barrie, and J. W. Valley (1997), Hydro-
1541 thermal alteration of oxygen isotope ratios in quartz pheno-
1542 crystals, Kidd Creek Mine, Ontario: Magmatic values are
1543 preserved in zircon, *Geology*, *25*, 1079–1082.
- 1544 Maas, R., P. D. Kinny, I. S. Williams, D. O. Froude, and
1545 W. Compston (1992), The Earth’s oldest known crust:
1546 A geochronological and geochemical study of 3900–4200
1547 Ma old detrital zircons from Mt. Narryer and Jack Hills, Wes-
1548 tern Australia, *Geochim. Cosmochim. Acta*, *56*, 1281–1300.
- 1549 Manning, C. E., S. J. Mojzsis, and T. M. Harrison (2006),
1550 Geology, age and origin of supracrustal rocks, Akilia, Green-
1551 land, *Am. J. Sci.*, *306*, 303–366.
- 1552 Markl, G. (2001), REE constraints on fractionation processes of
1553 massive-type anorthosites on the Lofoten Islands, Norway,
1554 *Mineral. Petrol.*, *72*, 325–351.
- 1555 Miller, R. L., and J. S. Kahn (1962), *Statistical Analysis in the*
1556 *Geological Sciences*, 483 pp., John Wiley, New York.
- 1557 Mojzsis, S. J., T. M. Harrison, and R. T. Pidgeon (2001),
1558 Oxygen-isotope evidence from ancient zircons for liquid
water at the Earth’s surface 4300 Myr ago, *Nature*, *409*, 1559
178–181. 1560
- Moorbath, S., M. J. Whitehouse, and B. S. Kamber (1997), 1561
Extreme Nd-isotope heterogeneity in the early Archaean: 1562
Fact or fiction? Case histories from northern Canada and 1563
West Greenland, *Chem. Geol.*, *135*, 213–231. 1564
- Nelson, D. R., B. W. Robinson, and J. S. Myers (2000), Com- 1565
plex geological histories extending for ≥ 4.0 Ga deciphered 1566
from xenocryst zircon microstructures, *Earth Planet. Sci.* 1567
Lett., *181*, 89–102. 1568
- Nemchin, A. A., R. T. Pidgeon, and M. J. Whitehouse (2006a), 1569
Re-evaluation of the origin and evolution of >4.2 Ga zircons 1570
from the Jack Hills metasedimentary rocks, *Earth Planet.* 1571
Sci. Lett., *244*, 218–233. 1572
- Nemchin, A. A., M. J. Whitehouse, R. T. Pidgeon, and C. Myer 1573
(2006b), Oxygen isotopic signature of 4.4–3.9 Ga zircons as 1574
a monitor of differentiation processes on the Moon, *Geochim.* 1575
Cosmochim. Acta., *70*, 1864–1872. 1576
- Nutman, A. P. (2006), Comment on “Zircon thermometer 1577
reveals minimum melting conditions on earliest Earth” II, 1578
Science, *311*, 779b, doi:10.1126/science.1120977. 1579
- Paces, J. B., and J. D. Miller (1993), Precise U-Pb ages of 1580
Duluth Complex and related mafic intrusions, northeastern 1581
Minnesota: Geochronological insights into physical, petro- 1582
genetic, and paleomagnetic and tectonomagnetic processes 1583
associated with the 1.1 Ga mid-continent rift system, *J. Geo-* 1584
phys. Res., *98*, 13,997–14,013. 1585
- Peck, W. H., J. W. Valley, S. A. Wilde, and C. M. Graham 1586
(2001), Oxygen isotope ratios and rare earth elements in 3.3 1587
to 4.4 Ga zircons: Ion microprobe evidence for high $\delta^{18}\text{O}$ 1588
continental crust and oceans in the early Archean, *Geochim.* 1589
Cosmochim. Acta., *65*, 4215–4229. 1590
- Peck, W. H., J. W. Valley, and C. M. Graham (2003), Slow 1591
oxygen diffusion rates in igneous zircons from metamorphic 1592
rocks, *Am. Mineral.*, *88*, 1003–1014. 1593
- Pettke, T., A. Audetat, U. Schaltegger, and C. A. Heinrich 1594
(2005), Magmatic-to-hydrothermal crystallization in the 1595
W-Sn mineralized Mole Granite (NSW, Australia). part II: 1596
Evolving zircon and thorite trace element chemistry, *Chem.* 1597
Geol., *220*, 191–213. 1598
- Pidgeon, R. T., and S. A. Wilde (1998), The interpretation of 1599
complex zircon U-Pb systems in Archaean granitoids and 1600
gneisses from the Jack Hills, Narryer gneiss terrane, Western 1601
Australia, *Precambrian Res.*, *91*, 309–332. 1602
- Reymer, A. P. S., and G. Schubert (1985), Continental volume 1603
and freeboard through geological time, *Nature*, *316*, 336– 1604
339. 1605
- Rubatto, D. (2002), Zircon trace element geochemistry: Parti- 1606
tioning with garnet and the link between U-Pb ages and 1607
metamorphism, *Chem. Geol.*, *184*, 123–138. 1608
- Ryerson, F. J., and E. B. Watson (1987), Rutile saturation in 1609
magmas: Implications for Ti-Nb-Ta depletion in orogenic 1610
rock series, *Earth Planet. Sci. Lett.*, *86*, 225–239. 1611
- Samsonov, A. V., M. M. Bogina, E. V. Bibikova, A. Y. Petrova, 1612
and A. A. Shchipansky (2005), The relationship between 1613
adakitic, calc-alkaline volcanic rocks and TTGs: Implications 1614
for the tectonic setting of the Karelian greenstone belts, Baltic 1615
Shield, *Lithos*, *79*, 83–106. 1616
- Sano, Y., K. Terada, H. Hidaka, K. Yokoyama, and A. P. Nutman 1617
(1999), Palaeoproterozoic thermal events recorded in the 1618
 ~ 4.0 Ga Acasta gneiss, Canada: Evidence from SHRIMP 1619
U-Pb dating of apatite and zircon, *Geochim. Cosmochim.* 1620
Acta, *63*, 899–905. 1621
- Schmitz, M. D., S. A. Bowring, and T. R. Ireland (2003), 1622
Evaluation of Duluth Complex anorthositic series (AS3) zir- 1623
con as a U-Pb geochronological standard: New high-prec- 1624

- 1625 sion isotope dilution thermal ionization mass spectrometry
1626 results, *Geochim. Cosmochim. Acta*, *67*, 3665–3672.
- 1627 Silverman, B. W. (1986), *Density Estimations for Statistics
1628 and Data Analysis, Monogr. Stat. Appl. Prob.*, vol. 26,
1629 175 pp., Chapman and Hall, London.
- 1630 Sun, S. S., and W. F. McDonough (1989), Chemical and
1631 isotopic systematics of oceanic basalts: Implications for
1632 mantle composition and processes, in *Magmatism in the
1633 Ocean Basins*, edited by A. D. Sanders and M. J. Norry,
1634 *Geol. Soc. Spec. Publ.*, *42*, 313–345.
- 1635 Taylor, H. P. (1968), The oxygen isotope geochemistry of
1636 igneous rocks, *Contrib. Mineral. Petrol.*, *19*, 1–71.
- 1637 Taylor, H. P., and S. M. F. Sheppard (1986), Igneous rocks:
1638 I. Processes of isotopic fractionation and isotope systematics,
1639 *Rev. Mineral. Geochem.*, *16*, 227–271.
- 1640 Tera, F., D. A. Papanastassiou, and G. J. Wasserburg (1974),
1641 Isotopic evidence for a terminal lunar cataclysm, *Earth Pla-
1642 net. Sci. Lett.*, *22*, 1–21.
- 1643 Trail, D., S. J. Mojzsis, and T. M. Harrison (2004), Inclusion
1644 mineralogy of pre-4.0 Ga zircons from Jack Hills, Western
1645 Australia: A progress report (abstract), *Geochim. Cosmo-
1646 chim. Acta.*, *68*, A743.
- 1647 Turner, G., T. M. Harrison, G. Holland, S. J. Mojzsis, and
1648 J. Gilmour (2004), Extinct Pu-244 in ancient zircons,
1649 *Science*, *306*, 89–91.
- 1650 Valley, J. W. (2003), Oxygen isotopes in zircon, *Rev. Mineral.
1651 Geochem.*, *53*, 342–385.
- 1652 Valley, J. W., J. R. Chiarenzelli, and J. M. McLelland (1994),
1653 Oxygen isotope geochemistry of zircon, *Earth Planet Sci.
1654 Lett.*, *126*, 187–206.
- 1655 Valley, J. W., W. H. Peck, E. M. King, and S. A. Wilde (2002),
1656 A cool early Earth, *Geology*, *30*, 351–354.
- 1657 Valley, J. W., I. N. Bindeman, and W. H. Peck (2003), Empiri-
1658 cal calibration of oxygen isotope fractionation in zircon,
1659 *Geochim. Cosmochim. Acta*, *67*, 3257–3266.
- 1660 Valley, J. W., et al. (2005), 4.4 billion years of crustal matura-
1661 tion: Oxygen isotope ratios of magmatic zircon, *Contrib.
1662 Mineral. Petrol.*, *150*, 561–580.
- 1663 Valley, J. W., A. J. Cavosie, B. Fu, W. H. Peck, and S. A.
1664 Wilde (2006), Comment on “Heterogeneous Hadean haf-
1665 nium: Evidence of continental crust at 4.4 to 4.5 Ga”,
1666 *Science*, *312*, 1139a, doi:10.1126/science.1125301.
- Vervoort, J. D., and J. Blichert-Toft (1999), Evolution of the
1667 depleted mantle: Hf isotope evidence from juvenile rocks
1668 through time, *Geochim. Cosmochim. Acta*, *63*, 533–556. 1669
- Watson, E. B., and D. J. Cherniak (1997), Oxygen diffusion in
1670 zircon, *Earth Planet. Sci. Lett.*, *148*, 527–544. 1671
- Watson, E. B., and T. M. Harrison (2005), New thermometer
1672 reveals minimum melting conditions on earliest Earth,
1673 *Science*, *308*, 841–844. 1674
- Watson, E. B., and T. M. Harrison (2006), Response to com-
1675 ments on “New thermometer reveals minimum melting con-
1676 ditions on earliest Earth”, *Science*, *311*, 779c, doi:10.1126/
1677 science.1121080. 1678
- Watson, E. B., D. A. Wark, and J. B. Thomas (2006), Crystal-
1679 lization thermometers for zircon and rutile, *Contrib. Mineral.
1680 Petrol.*, *151*, 413–433. 1681
- Whitehouse, M. J., and B. S. Kamber (2002), On the over-
1682 abundance of light rare earth elements in terrestrial zircons
1683 and its implication for Earth’s earliest magmatic differentia-
1684 tion, *Earth Planet. Sci. Lett.*, *204*, 333–346. 1685
- Whitehouse, M. J., and B. S. Kamber (2003), A rare earth
1686 element study of complex zircons from early Archaean
1687 Amitsoq gneisses, Godthåbsfjord, south-west Greenland,
1688 *Precambrian Res.*, *126*, 363–377. 1689
- Whitehouse, M. J., and B. S. Kamber (2005), Assigning dates
1690 to thin gneissic veins in high-grade metamorphic terranes: A
1691 cautionary tale from Akilia, southwest Greenland, *J. Petrol.*,
1692 *46*, 291–318. 1693
- Whitehouse, M. J., and J. P. Platt (2003), Dating high-grade
1694 metamorphism: Constraints from rare-earth elements in
1695 zircon and garnet, *Contrib. Mineral. Petrol.*, *145*, 61–74. 1696
- Wiedenbeck, M., et al. (2004), Further characterisation of the
1697 91500 zircon crystal, *Geostand. Geoanal. Res.*, *28*, 9–39. 1698
- Wilde, S. A., J. W. Valley, W. H. Peck, and C. M. Graham (2001),
1699 Evidence from detrital zircons for the existence of continental
1700 crust and oceans 4.4 Ga ago, *Nature*, *409*, 175–178. 1701
- Young, E. D., M. L. Fogel, D. Rumble, and T. C. Hoering
1702 (1998), Isotope-ratio-monitoring of O₂ for microanalysis of
1703 ¹⁸O/¹⁶O and ¹⁷O/¹⁶O in geological materials, *Geochim. Cos-
1704 mochim. Acta*, *62*, 3087–3094. 1705
- Zheng, Y. F., B. Fu, B. Gong, and L. Li (2003), Stable isotope
1706 geochemistry of ultrahigh pressure metamorphic rocks from
1707 the Dabie-Sulu orogen in China: Implications for geody-
1708 namics and fluid regime, *Earth Sci. Rev.*, *62*, 105–161. 1709